Williams-Jones, A. E., and Vasyukova, O. V., 2022,
Niobium, Critical Metal and Progeny of the Mantle: Economic Geology, v. doi:10.5382/econgeo.4994.

NIOBIUM, CRITICAL METAL AND PROGENY OF THE MANTLE

A.E. Williams-Jones and O.V. Vasyukova

Department of Earth and Planetary Sciences, McGill University, 3450 University Street Montréal, Québec, Canada, H3A 0E8

ABSTRACT

Niobium is a critical metal in high demand because of technological advances and the supply risk created by the fact that over 90 % of its production is by a single country (Brazil). In this paper, we review the geology of the deposits that are currently being mined and other potentially economic deposits as well as develop models for their genesis. With the exception of the Lovozero deposit (Russia), which is hosted by a layered silica-undersaturated alkaline igneous complex, all the deposits that are currently being mined for niobium are hosted by carbonatites, and most of the deposits with economic potential are also hosted by carbonatites. Niobium owes its concentration in carbonatites and alkaline igneous rocks to its highly incompatible nature and the small degree of partial melting of the mantle required to generate the corresponding magmas. The primary control on the concentration of niobium to economic levels in alkaline silicate magmas is fractional crystallization, partly prior to but mainly after emplacement. In the case of silica-undersaturated magmas, the final residue saturates in minerals like eudialyte and loparite to form niobium-rich horizons in the layered complexes that crystallize from these magmas. The final residue, in the case of silica-saturated magmas, crystallizes the pegmatites that are the hosts to the economic niobium mineralization, which commonly takes the form of pyrochlore. In contrast, carbonatitic magmas undergo little to no fractional crystallization prior to emplacement. Moreover, fractional crystallization at the site of emplacement has minimal impact on the concentration of niobium to economic levels. Instead, we propose that the metasomatic interaction of the carbonatitic magmas with their hosts to form rocks like phlogopitite (glimmerite), consumes much of the magma, leaving behind a phoscoritic residue from which pyrochlore crystallizes in amounts sufficient to form economic deposits. Although many niobium deposits display evidence of intense hydrothermal alteration, and there can be major changes in the niobium mineralogy, the extremely

low solubility of niobium in aqueous fluids at elevated temperature precludes significant mobilization and, thus, enrichment of the metal. However, weathering of carbonatite-hosted niobium deposits leads to supergene enrichment (due largely to the dissolution of the carbonate minerals) that can double the niobium grade and make subeconomic deposits economic. Pyrochlore is the principal niobium mineral in these laterite-hosted deposits, although its composition differs considerably from that in the primary mineralization. This paper evaluates the processes that appear to be responsible for the genesis of niobium ores and provides a framework that we hope will guide future in-depth studies of niobium deposits and lead to more effective strategies for their successful exploration and exploitation.

INTRODUCTION

Niobium is a critical metal because it is an essential component in many high-strength corrosion-resistant low-alloy (HSLA) steels and superalloys, and because of its high supply risk; a single country, Brazil, is responsible for over 90 % of global niobium production. Indeed, it has the highest combination of supply risk and economic importance indices of any element except, magnesium (Rachidi et al., 2021). Currently, approximately 75 % of niobium is consumed as ferroniobium HSLA steels for use in pipelines and transportation, and for structural applications (Schulz et al., 2017). A significant proportion of the niobium supply is used in nickel-, cobalt-, and iron-based superalloys for high temperature applications, including gas turbines and heat-resisting combustion equipment. In the longer term, other applications, notably in superconducting magnetic coils for MRIs and magnetic levitation rail transport systems, are expected to produce an even greater demand for niobium. During the next five years, demand for this metal is predicted to increase at a compounded annual rate of 6 % (https://www.businesswire.com). This demand and the fact that three deposits control the supply chain have led a number of countries to rank niobium near the top of their lists of critical materials, and this is fuelling exploration for new niobium resources.

The supply of niobium is dominated by a single deposit, the Araxá carbonatite-hosted niobium deposit in Brazil. This deposit contains 26.5×10^6 metric tonnes of Nb_2O_5, of which 11.5×10^6 metric tonnes is lateritic ore grading 2.48 wt.% Nb_2O_5 and 15×10^6 metric tonnes is in the unweathered carbonatite and has a grade of 1.6 wt.% Nb_2O_5 (Cordeiro et al., 2011). The second largest deposit currently being exploited is hosted by the St Honoré carbonatite, Canada, with a reserve of 2.6×10^6

metric tonnes of Nb_2O_5 in ores grading 0.42 wt.% Nb_2O_5 (Vallieres et al., 2013), followed by the carbonatite-hosted Catalão I deposit in Brazil, containing $559x10^3$ metric tonnes of Nb_2O_5 in ores grading 1.17 wt.% (Cordeiro et al., 2011). These three deposits are responsible for 99 % of annual global niobium production, i.e., ~63,000 metric tonnes of niobium (Schulz et al., 2017). Significantly, the carbonatite-associated Bayan Obo deposit (China), which is the World's largest supplier of REE, has reserves of $1.0x10^6$ metric tonnes of Nb_2O_5 that could be exploited (Berger et al., 2009). In addition to carbonatites, alkaline igneous rocks are a potentially important source of niobium. Indeed, niobium is currently being mined from the Lovozero layered alkaline igneous complex (Russia) at an annual rate of ~2400 metric tonnes of Nb_2O_5 as a by-product of the mining of the REE (Schulz et al., 2017). Other layered complexes that contain significant resources of niobium include the Motzfeldt layered complex (Greenland) with $1.6x10^6$ metric tonnes of Nb_2O_5 in ores grading 0.46 wt.% Nb_2O_5 and the Nechalacho layered intrusive suite (Canada) with an indicated and inferred reserve of $1.1x10^6$ metric tonnes of Nb_2O_5 in ores grading 0.36 wt.% (Schulz et al., 2017). Niobium is also present in significant proportions in the pegmatites associated with peralkaline granites. For example, the Strange Lake (Canada), Khaldzan Buregtey (Mongolia) and Baerzhe (China) granites host resources of $500x10^3$, $560x10^3$ and $260x10^3$ metric tonnes of Nb_2O_5 in ores with grades of 0.34, 0.14 and 0.26 wt.% Nb_2O_5, respectively (Kovalenko et al., 1995, Yang et al., 2014, Vasyukova and Williams-Jones, 2018).

In this paper, we review the discovery of niobium, its chemical behavior, its mineralogy, the nature of representative niobium deposits and the processes that concentrate niobium to economic and potentially economic levels. Our evaluation of the latter starts by considering the origin of carbonatites and alkaline igneous rocks and the processes that control the evolution of the corresponding magmas. In so doing, we trace the path of niobium through this igneous evolution, and then continue our evaluation by examining the subsolidus processes (including weathering) that conspire to form economic deposits.

DISCOVERY OF NIOBIUM

Niobium was discovered in 1801 by Charles Hatchet, an English mineralogist and chemist. He had been examining minerals in the British Museum and came across a specimen of an unnamed heavy black mineral that resembled "Siberian chromate of iron" on which he had been conducting experiments (Hatchett, 1802). Hatchett expanded his experiments to include this specimen, which

had been part of the collection of John Winthrop, the first governor of Connecticut, an avid mineral collector. After discovering that, except for the dissolution of some iron, the mineral was largely insoluble in hydrochloric, nitric and sulfuric acids, Hatchett fused a small proportion of the mineral repeatedly in potassium carbonate, dissolved the latter in boiling water and produced a white precipitate by mixing the solution with nitric acid. After trying unsuccessfully to dissolve the white precipitate in a variety of acids and conducting a number of other tests, Hatchett concluded that he had discovered a new metallic "earth" (Hatchett, 1802). He named the new earth (element) "Columbium" because of its country of origin; the mineral was named columbite. Whether columbium refers to Columbia, the female personification of the United States, or Christopher Columbus is unknown.

A year after Hatchett discovered columbium, Anders Ekeberg, a Swedish chemist, discovered a metal with very similar properties in a mineral from Ytterby, which he named "Tantalum" after the Greek demi-god Tantalus (Ekeberg, 1803). There was considerable debate over whether columbium and tantalum were the same metal (Wollaston, 1809) until the matter was resolved by the German chemist Heinrich Rose, who showed that the earth discovered by Hatchett (columbium) was a mixture of tantalum and a new earth that he named "Niobium" after Niobe, a daughter of Tantalus (Rose, 1844). Niobium metal was first extracted in 1864 by Christian Blomstrand, a Swedish chemist and mineralogist (Kauffman, 1975). This metal was referred to as columbium (Cb) in North America and niobium (Nb) in Europe until 1949, when the International Union of Pure and Applied Chemistry (IUPAC) formally adopted the name niobium in a quid pro quo involving tungsten and wolfram.

PROPERTIES OF NIOBIUM

Niobium is a transition metal in Group 5 of the Periodic table with the electronic configuration [Kr] $5s^1$ $4d^4$. In nature, it occurs almost exclusively as the stable isotope ^{93}Nb. It also has two radioisotopes, ^{92}Nb with a half-life of 3.47×10^7 and ^{94}Nb with a half-life of 2.03×10^4. It is paramagnetic, and has a melting temperature of 2,477 °C, a boiling point of 4,744 °C, a Vickers hardness of 1320 MPa and a density of 8.57 g/cm^3. Although niobium may occur in several oxidation states, in nature it is present exclusively in the +5 state. In minerals, it occurs dominantly in octahedral coordination with an ionic radius of 0.64 Å. Niobium has an electronegativity of 1.6, and the second and third ionization energies are 1,351 and 2,415 kJ/mol, respectively. Potentially

one of the most interesting properties of niobium is that it is a superconductor at temperatures up to 9.25 K. Indeed, its upper temperature limit of superconductivity is higher than that of any other metal, making it a key component of MRIs and particle accelerators. It will also be essential for the future implementation of magnetic levitation rail transport.

MINERALOGY

Niobium is a lithophile element and, thus, has a strong affinity for oxygen, with which it bonds to form oxyanions, notably, NbO_3^- and NbO_4^{3-}. Two common niobium-bearing minerals containing these anions are columbite-(Fe) and fergusonite-Y (Table 1). The oxyanion NbO_3^- is also an essential component of the main niobium ore mineral, pyrochlore, which has the generalized formula $A_{2-m}B_2X_{6-w}Y_{1-n}$ (m, w and n refer to vacancies). The A-site of this mineral contains cations in 8-fold coordination, most commonly Ca and Na, but also Ba, Sr, Pb, Fe^{2+}, Mn, the REE, U^{4+} and Th, and may include a vacancy, or H_2O (Atencio et al., 2010). The B-site has 6-fold coordination and is mainly occupied by Nb (it can also contain Ta, Zr, Hf, Ti, W, Si and Fe^{3+}). The X-site is typically occupied by O but can also contain OH and F, and the Y-site may be occupied by an anion (e.g., OH^-, F^- or Cl^-), H_2O, a vacancy, or a large cation, such as K^+ and Rb^+ (Atencio et al., 2010). Other niobium minerals include aeschynite, biotite, betafite, euxenite-(Y), fersmite, ixiolite, loparite, lueshite, niobian rutile, niobian brookite, niocalite, samarskite-(Yb), tapiolite and wodginite (Table 1). Among these other minerals only loparite is being mined for niobium, but aeschynite is potentially a major source of niobium at Bayan Obo. The only other significant niobium ore minerals are niobian rutile and niobian brookite, which occur as supergene phases, notably, in the Seis Lagos deposit in Brazil, where they are the principal potential source of niobium in a laterite resource (Giovannini, 2013) and niocalite, which is the principal ore mineral in the Bond Zone of the Oka carbonatite (Gold, 1963).

The main ore mineral for niobium in the three deposits that are responsible for most of the World's niobium production is pyrochlore the composition of which varies considerably amongst the deposits. Thus, at Araxá (Brazil), the main primary pyrochlore variety is barium-bearing calciopyrochlore, whereas the supergene pyrochlore (the ore mineral currently being mined) is bariopyrochlore (Issa Filho et al., 2002b). The same is true of the primary and supergene ores of Catalão 1, Brazil (Cordeiro et al., 2011). In contrast, at St Honoré (Canada), the primary pyrochlore evolved from an early U-Ta-Zr-Th-bearing calciopyrochlore to a late fluorcalciopyrochlore

(unpublished data). Furthermore, in parts of the deposit, the pyrochlore was altered hydrothermally to columbite-(Fe) in volumes sufficient to make it an important subordinate niobium ore mineral (Tremblay et al., 2017).

NIOBIUM DEPOSITS

Because of its high charge, niobium is a highly incompatible element and, during partial melting of the mantle, it partitions strongly into the first liquids that form. Consequently, it reaches its highest concentration in carbonatites and alkaline igneous rocks. These are the hosts to all economic or potentially economic primary niobium deposits.

Carbonatite-hosted niobium deposits

As mentioned in the introduction, global niobium production is dominated by three carbonatite-hosted deposits, namely, Araxá, Catalão and St Honoré. In each of these deposits, pyrochlore is the main ore mineral. However, whereas the niobium mined at St Honoré is hypogene, at both Catalão and Araxá, all the current production is from laterites that overlie carbonatites.

Araxá

Despite the importance of the Araxa deposit and the fact that it has been mined for several decades, there is relatively little published information on the geology of the deposit; the most comprehensive paper on it is that of Traversa et al. (2001). The Araxá complex is a member of the 80-90 Ma Alto Paranaiba Alkaline Igneous Province in south-eastern Brazil, which is interpreted to have formed as a result of the partial melting of the Trindade mantle plume (Gibson et al., 1995). The complex is 4.5 km wide, roughly circular in plan, and was emplaced in a group of Proterozoic quartzites and schists of the Araxá group (Fig. 1a). It has been described by Traversa et al. (2001) as comprising a large mass of glimmerite containing domains in which there are swarms of concentric and radial dykes of dolomite carbonatite, much less commonly calcite carbonatite and minor phoscorite (Traversa et al., 2001). The term “glimmerite”, however, is misleading. These rocks would be better described as ultramafic rocks (clinopyroxenites and peridotites) that have been variably altered to phlogopite and tetraferriphlogopite. Indeed, Traversa et al. (2001) subdivided them into mica-rich (phlogopitized) rocks with relicts of clinopyroxene and olivine and mica-olivine pyroxenites. They also note that olivine is much more important in the mica-rich rocks and that clinopyroxene is the dominant ferromagnesian mineral in the second group of rocks,

in which the mica is a primary mineral. We, therefore, infer that the mica-rich rocks comprise highly phlogopitized peridotite and that the second group of rocks consists mainly of relatively unaltered clinopyroxenite. The calcite carbonatite dykes are relatively coarse-grained, and contain some dolomite in addition to calcite, and variable proportions of phlogopite, arfvedsonite, magnetite, apatite and minor pyrochlore. In contrast, the dolomite carbonatite dykes are fine-grained and contain minor calcite. They also contain phlogopite, which is locally abundant, magnetite, apatite and significant pyrochlore. An unusual feature of the dolomite carbonatite is that the Ba-carbonate mineral, norsethite ($BaMg(CO_3)_2$), is commonly present and locally abundant. The phoscorite dykes are mainly associated with calcite carbonatite and are dominated by the mineral assemblage apatite-phlogopite-magnetite. The complex is surrounded by a 2.5 km wide aureole, in which the host quartzites and schists were fenitized (alkali feldspar and sodic amphibole).

The pyrochlore occurs dominantly in the dolomite carbonatite and glimmerite (Traversa et al., 2001). Unfortunately, there is almost no published information on the composition of pyrochlore in the carbonatite. However, scanning electron microscope images and energy dispersive spectra of laterite-hosted pyrochlore in Issa Filho et al. (2002a) showing calciopyrochlore with minor Ba and Th partly replaced by bariopyrochlore suggest that the primary pyrochlore was calciopyrochlore. The secondary bariopyrochlore, which is the principal ore mineral in the laterite and contains ~15 wt.% BaO, was interpreted by Issa Filho et al. (2002a) to be the product of weathering.

Catalão I

The Catalão I deposit is hosted by a phoscorite-carbonatite complex and overlying laterite located at the northern end of the Alto Paranaiba Igneous Province (Cordeiro et al., 2011, Oliveira et al., 2017). The complex is 6 km wide and comprises a core of phoscorites and subordinate dolomite carbonatites surrounded by variably phlogopitized ultramafic rocks (glimmerites) and lesser proportions of phoscorites/carbonatites that were emplaced in schists and quartzites of the Araxá Group (Fig. 1b). The earliest phoscorites are olivine-bearing and occur as small plugs and dykes. They were intruded by phlogopite phoscorites, referred to by Cordeiro et al. (2010) as nelsonites, and dolomite carbonatites that also occur as small plugs and dykes. These two rock types are intimately related, as shown by the fact that the nelsonite contains small pockets of dolomite

carbonatite and small pockets of nelsonite are present in the dolomite carbonatites. The surrounding ultramafic rocks comprise dunite and perovskite-rich clinopyroxenite (bebedourite). An aureole of fenite up to several hundred meters wide surrounds the complex.

The primary niobium mineralization is concentrated mainly in the nelsonites, but some dolomite carbonatite intrusions also contain significant niobium. It occurs primarily as Na-bearing calciopyrochlore and much less commonly as natropyrochlore (Cordeiro et al., 2011, Guarino et al., 2017). Some crystals of calciopyrochlore and natropyrochlore have rims of Ba- and vacancy-rich pyrochlore. They may also be enriched in the light REE (Guarino et al., 2017). Although the overall grade of primary mineralization is ~1 wt.% Nb_2O_5, individual nelsonite dykes may contain as much as 50 vol.% pyrochlore, i.e., ~40 wt.% Nb_2O_5. As is the case at Araxá, the supergene mineralization is dominated by bariopyrochlore (Cordeiro et al., 2011).

St Honoré

The St Honoré carbonatite was emplaced at 571 ± 5 Ma (McCausland et al., 2009) in the ~1 Ga Grenville Metamorphic Province of Québec, Canada (Tremblay et al., 2017)). In contrast to the Araxá and Catalão I carbonatite complexes, ultramafic rocks and phoscorites are absent at St Honoré, and the phlogopitites are the products of the alteration of syenite. The St Honoré complex is roughly elliptical in plan (2x3 km) and comprises a core of ferrocarbonatite, which contains a potential REE resource, a mantle consisting dominantly of dolomite and calcite carbonatites and an incomplete rim of calcite carbonatite (Fig. 2a). These units are surrounded by syenite. The textural relationships among the various carbonatite units are complex, largely because the carbonatites are not single intrusions. Instead, each of them is a composite of a large number of dykes and plugs ranging in width from a few centimeters to several meters (Vasyukova and Williams-Jones, 2022). A conspicuous feature of the complex is that the contact between the carbonatite and the syenite is commonly separated by a zone of variably phlogopitized syenite reaching tens of meters in thickness, which is locally magnetite-rich. Significantly, fragments of variably phlogopitized syenite (Fig. 3) are present in the carbonatite for considerable distances from this contact and locally may comprise > 50% of the carbonatite.

The niobium mineralization is concentrated in dolomite and calcite carbonatites in the southwest part of the complex, particularly, where they comprise high proportions of phlogopitized syenite

fragments or are close to the contact with phlogopitite; some of the highest concentrations of niobium occur at the contact between this unit and carbonatite. The description that follows is based on ongoing research of the niobium mineralized units by the authors. The mineralization takes the form of pyrochlore and subordinate columbite-(Fe) that occur as pseudomorphs after pyrochlore (Fig. 4). These minerals occur in carbonatites that display distinct millimetric to centimetric subvertical layering (Fig. 3c and d). The pyrochlore and columbite-(Fe) are concentrated in apatite-rich layers that contain variable proportions of magnetite and phlogopite. Minor pyrochlore is also present in the intervening carbonate-rich layers. Many of the pyrochlore crystals contain a calciopyrochlore core, which is enriched in U, Ta, Zr and Th, and an overgrowth of oscillatory zoned calciopyrochlore with a large natropyrochlore component (Fig. 4). The remaining crystals are compositionally the same as the overgrowths. Pyrochlore is also abundant in the magnetite-rich phlogopitites. Compositionally, this pyrochlore is very similar to the calciopyrochlore rims in the carbonatite (Fig. 4). In the north-eastern part of the mineralized carbonatite, there are large domains in which the pyrochlore has been altered to columbite-(Fe) that generally preserves the shape of the precursor pyrochlore (Fig. 4f).

Other carbonatite-hosted niobium deposits

Among the other carbonatite complexes that have been mined for niobium, the Lower Cretaceous **Oka** carbonatite complex (Canada) is the best known. This deposit (A and D zones), which was mined from 1961 to 1977, had a measured and indicated reserve of 57 Mt of ore grading 0.38 wt.% Nb_2O_5 (https://gq.mines.gouv.qc.ca/documents/examine/GM12938/GM12938.pdf). The Oka carbonatite (7.2x2.4 km) consists dominantly of two lobes of calcite carbonatite and subordinate arcuate bodies of ultramafic and ultrabasic rocks that are concentrated towards the margins of the lobes (Fig. 2b). There is also a small proportion of dolomite carbonatite in the northernmost part of the northern lobe. The silicate rocks have been subdivided by Gold (1963) into three main units, namely, ijolite (melteigite-urtite), okaite-jacupirangite and alnöite. The ijolite is the most important of these units, making up over 85 % of the silicate rocks, and was locally phlogopitized. Okaite-jacupirangite is the next most important unit and is concentrated in the outer part of the northern lobe. Compositionally, this unit varies from melilite-rich okaite to titanaugite-rich jacupirangite with minor proportions of nepheline, magnetite, apatite, calcite and perovskite. The final unit, alnöite, is restricted to the western margins of the southern lobe. It consists of phenocrysts of

olivine, augite and phlogopite in a calcite-rich matrix comprising these minerals plus melilite, apatite, nepheline and perovskite.

Economic niobium mineralization occurs in three zones near the eastern (A and D zones), western (Bond Zone) and northern (Manny Zone) margins of the northern lobe of the complex. Only the A and D zones, however, were mined. The main niobium minerals are pyrochlore, niobian perovskite and niocalite. However, pyrochlore was the only niobium mineral recovered during mining operations. The occurrence of niocalite is restricted to the Bond Zone, where it reaches concentrations of 10 vol. % (Gold, 1963). Carbonatites containing the highest concentrations of the three niobium minerals are characterized by thin layers alternately rich in calcite and in apatite-magnetite-biotite. The latter layers host most of the pyrochlore and perovskite. Niocalite, which, as noted above, is restricted to the Bond Zone, is concentrated mainly in the calcite-rich layers. Close to ijolite and particularly phlogopitized ijolite, the proportions of apatite and magnetite in the coarse-grained carbonatite increase considerably, as do the proportions of pyrochlore and perovskite. Indeed, these rocks have the highest concentration of Nb_2O_5 in the mineralized zones. The pyrochlore varies considerably in composition and includes Ca-, Ce-, Th-, U-, Ti- and Zr-rich varieties that Zurevinski and Mitchell (2004) have interpreted to reflect variable A-site substitution of Ca and Na by Ce, Th and U and B-site substitution of Nb and Ti by Zr. The perovskite varies in composition from near end member perovskite to a mineral with a composition close to that of latrappite ($Ca_2NbFe^{3+}O_6$). As a result, it may contain over 40 wt.% Nb_2O_5 and as little as 10 wt.% TiO_2 (Gold, 1963).

The only other carbonatite that, to our knowledge, has been an important source of niobium is the **Lueshe** carbonatite in the Democratic Republic of Congo (DRC). This deposit contained a resource of 30 Mt grading 1.34 wt.% Nb_2O_5 and was mined intermittently between 1984 and 2004. In contrast to the two preceding deposits, the niobium ore is contained entirely in laterite developed above calcite carbonatite in a carbonatite-syenite complex. The 516 Ma complex is ~3 km x 1.5 km in plan and comprises cancrinite syenite (~40 % of the plan area), calcite carbonatite (~40 % of the plan area) and dolomite carbonatite (~20 % of the plan area). These units are interpreted to have been intruded in the order listed here (Maravic et al., 1989). There are also small bodies of sodic pyroxenite along the contacts between calcite carbonatite and cancrinite syenite. The host rocks, which comprise quartzites and quartz mica schists, have been altered to sodic pyroxene-

sodic amphibole-albite-bearing fenite adjacent to the calcite carbonatite and dolomite carbonatite. Primary niobium mineralization occurs as calciopyrochlore that is concentrated in a fine-grained laminated facies of the calcite carbonatite at its contact with the cancrinite syenite (Maravic et al., 1989).

The laterite-hosted niobium ores reach their highest grade in the upper, crandallite-rich (crandallite is a weathering product of apatite) part of the 30-150 m thick laterite profile and decrease in Nb grade to the base of the profile where residual apatite and K-feldspar overlie the fresh carbonatite. The main laterite minerals are goethite and montmorillonite. Pyrochlore is the dominant ore mineral; there is also minor lueshite and niobian rutile. At the top of the profile, pyrochlore has the composition of bariopyrochlore, and A-site vacancies are at a minimum (Fig. 5). With increasing depth in the profile, the proportion of A-site vacancies in the pyrochlore increases significantly and reaches a maximum in the middle of the profile. This pyrochlore corresponds to kaliopyrochlore, a variety of pyrochlore unique to the Lueshe deposit. With further increase in depth, the proportion of K in the pyrochlore decreases and the proportion of Sr increases, leading to strontiopyrochlore being the main pyrochlore variety near the base of the laterite. These changes in pyrochlore composition with depth are interpreted by Wall et al. (1996) to represent progressive leaching of the A-site of the mineral by acidic weathering fluids and the uptake of Ba and subsequently K, both due to the breakdown of alkali feldspar present in unaltered carbonatite. The concentration of Ba in the pyrochlore at the top of the profile and K lower down is interpreted by them to be a result of the greater mobility of K. As Sr is likely to have been released by weathering of the carbonatite, its concentration in pyrochlore is highest at the base of the profile, i.e., closest to the least weathered carbonatite.

Among carbonatites with significant niobium mineralization that have not been mined, the most important is the **Seis Lagos** carbonatite, Brazil, with reserves of 2898 Mt at 2.81 wt% Nb_2O_5. Other potentially important carbonatites include the **Mt Weld** carbonatite, Australia (273 Mt at 0.9 wt% Nb_2O_5) and the **Aley** carbonatite, Canada (285.8 Mt at 0.3 wt% Nb_2O_5).

The Mesozoic **Seis Lagos** deposit is the largest niobium deposit in the World. Unlike the Araxá and Catalão laterite-hosted ores, however, the laterite at Seis Lagos is largely devoid of pyrochlore and, instead, most of the niobium is in the form of secondary niobian rutile and niobian brookite.

The Seis Lagos carbonatite is an isolated intrusion located in the 1.8 Ga Guyana Shield in North-Eastern Brazil. The intrusion is not exposed and has only been intersected in a single drillhole. Based on examination of the drill core from this intersection, the intrusion was interpreted by Giovannini et al. (2017) to be a siderite carbonatite containing subordinate barite and gorceixite [$BaAl_3(PO_4)(PO_3OH)(OH)_6$] plus minor monazite and pyrochlore. Assays of the core yielded niobium concentrations between 646 and 7667 ppm Nb_2O_5. The overlying laterite is over 100 m in thickness and has been subdivided into eight units (Fig. 6). The main minerals making up the laterite are hematite and goethite, which decrease and increase in proportions downwards, respectively. The only other mineral reported to be present in appreciable proportions is hollandite ($BaMn_8O_{16}$), which forms a roughly 10 m thick manganiferous laterite half-way down the profile. Niobium concentrations are highest in the goethite-rich laterite (brown laterite) at the base of the profile, where they reach values in excess of 8 wt% Nb_2O_5, and are lowest in the manganiferous laterite. In the upper part of the profile, concentrations of niobium parallel those of titanium, consistent with the observation that niobium is concentrated almost exclusively as niobian rutile and niobian brookite. In the basal, Nb-rich, goethite laterite, however, niobium concentration is decoupled from that of titanium, which is considerably lower and niobian rutile is accompanied by ceriopyrochlore. An interesting feature of the profile is that there is a progressive increase in niobium content from the base of the manganiferous laterite through the lower purple laterite to a maximum a third of the way into the brown laterite (Fig. 6). Given that this build-up in niobium concentration is near the bottom of the profile and the source of the niobium was the underlying carbonatite, it is attractive to propose that the weathering occurred in two stages. In the first stage, the carbonatite was leached, leaving behind a residue that was greatly enriched in pyrochlore (the primary niobium mineral in the carbonatite), silicate (e.g., biotite, amphibole and olivine), oxide (e.g., magnetite) and phosphate (e.g., apatite) minerals. During the second stage, these residual minerals became the "source rock" for the development of a laterite in which the breakdown of Ti-bearing magnetite and pyrochlore led to the formation of niobian rutile and niobian brookite.

The **Mt Weld** deposit (Australia) contains its potentially exploitable niobium resource in a laterite that overlies a Proterozoic carbonatite in the central part of the Eastern Goldfields Alkaline Igneous Province of the Yilgarn craton (Middlemost, 1990). The intrusion is pipe-like (~12 km^2 in plan) with a ~0.5 km wide rim of glimmerite and was emplaced in mafic to ultramafic volcanic rocks (greenstones). Calcite carbonatite containing significant proportions of olivine, apatite, magnetite

and biotite was intruded first, followed by dolomite carbonatite containing apatite, magnetite, phlogopite and pyrochlore. The proportions of non-carbonate minerals in the latter are highly variable and these minerals generally occur as layers and lenses. Biotite is concentrated mainly in the glimmerite zone that surrounds the intrusion. The primary carbonatite is overlain by a 40-60 m thick layer of laterite and, in turn, a 15-60 m layer of lacustrine sediments and alluvium (Lottermoser, 1990). The laterite has been subdivided into a discontinuous apatite-rich zone up to 20 m thick at the base and an alumino-phosphate-rich zone characterized by the presence of crandallite and goyazite-gorceixite group minerals. Niobium contents are highest in the alumino-phosphate zone, reaching up to 4 wt.% Nb_2O_5 vs. 0.7 wt.% Nb_2O_5 in the apatite-rich zone. The bulk of the niobium occurs as pyrochlore, although there are small proportions of niobian rutile and niobian ilmenite.

In most primary pyrochlore crystals, the A-site is filled largely by roughly equal proportions of Ca and Na, and vacancies are rare (Lottermoser, 1990). Some crystals, however, are characterized by an A-site that contains up to 10 wt.% of U and ~40 % vacancies. The B-site is generally occupied entirely by Nb, although in some cases it may contain >5 wt.% of Ta. In contrast to the primary pyrochlore, the laterite-hosted pyrochlore is strongly enriched in Sr throughout the laterite profile reaching a maximum of 18 wt.% SrO at the interface between the alumino-phosphate- and apatite-rich layers (Fig. 7). The laterite-hosted pyrochlore is also enriched in Ce (Ce^{4+}), which reaches its highest concentration in the upper part of the alumino-phosphate-rich layer (> 20 wt.% CeO_2). All the laterite-hosted pyrochlore is characterized by A-site vacancies (20-60 %), and although there is no obvious correlation of A-site vacancy with pyrochlore composition, it may be significant that the highest proportion of vacancies is for the most Sr-rich (and Ce-poor) pyrochlore (Lottermoser and England, 1988).

The **Aley** carbonatite is of Devonian age, i.e., ~370 Ma (Chakhmouradian et al., 2015), and was intruded into Cambro-Ordovician carbonate and siliciclastic metasedimentary rocks during a period of extension and rifting in the development of the Foreland fold-and-thrust margin of Western Canada. The intrusion is roughly triangular in shape (~7 km^2) and consists dominantly of calcite carbonatite that, according to Chakhmouradian et al. (2015), was altered to dolomite carbonatite, except at the edge of the intrusion (minor primary dolomite carbonatite is also observed). The carbonatite contains up to 10 % apatite and variable proportions of phlogopite and

magnetite (Yelland, 2016). Mineral layering is common and is distinguished mainly by planar aggregates of apatite, magnetite and, locally, niobium minerals. Although the minerals in the aggregates are interpreted to be cumulates, the layering has been attributed to post-emplacement deformation (Chakhmouradian et al., 2015). The carbonatite is surrounded by an aureole up to several hundred meters in width, in which the host rocks have been metasomatically altered to amphibole- or biotite-rich (phlogopitite) fenites. The niobium mineralization comprises pyrochlore, columbite-(Fe) and fersmite (Yelland, 2016). Two zones of mineralization (layers of magnetite, apatite and niobium minerals), the Central and Saddle Zones, have been identified, although the resource referred to above is entirely in the Central Zone, where fersmite is the principal ore mineral and is accompanied by subordinate columbite-(Fe) and minor pyrochlore. The fersmite is interpreted to have replaced pyrochlore and/or columbite-(Fe) during dolomitization (Chakhmouradian et al., 2015) and is concentrated in layers together with magnetite, apatite and phlogopite (Yelland, 2016).

A potentially important niobium deposit associated with carbonatite is the **Bayan Obo** deposit in China, which is hosted by magnetite-aegirine-rich rocks considered to have formed as a result of the interaction of carbonatite-derived hydrothermal fluids with carbonate rocks of disputed origin (magmatic or sedimentary; Smith et al., 2015). Although this deposit was mined initially for iron and is currently the World's largest REE deposit, it also contains a niobium resource of ~1690 Mt of ore grading 0.16 Nb_2O_5 (Smith and Spratt, 2012). The niobium takes the form of aeschynite and subordinate pyrochlore, which occur in the REE mineralized fluorite-bearing aegirine-magnetite rocks. The aeschynite and pyrochlore, however, post-date the main REE minerals, bastnäsite-(Ce) and monazite-(Ce), and occur in spatial/temporal association with riebeckite, fluorite, barite and quartz. Compositionally, the aeschynite is a Ce- and Nd-rich variety, containing similar amounts of both elements (~12 wt.% REE_2O_3). These minerals were subsequently altered to baotite and bafertisite ($Ba_2Fe^{2+}_4Ti_2(Si_2O_7)_2O_2(OH)_2F_2$). Based on an earlier study of fluid inclusions (Smith and Henderson, 2000), Smith and Spratt (2012) concluded that the niobium mineralization took place at a temperature of 250-300 ºC and a pressure ~1 kbar from carbonatite-related fluids containing between 20 to 30 wt.% NaCl eq.

Niobium deposits hosted by alkaline igneous rocks

Niobium occurs in significant concentrations in a number of silica-saturated and silica-undersaturated alkaline igneous complexes, notably, Lovozero, Khibiny, Ilímaussaq, Motzvelt, Nechalacho, Khaldzan Buregtey, Baerzhe and Strange Lake. In all cases, the concentration of niobium is subordinate to those of the REE. Here, we describe the Lovozero (the only alkaline igneous complex currently being mined for niobium) and Nechalacho complexes as representatives of the silica-undersaturated group of intrusions enriched in niobium and Strange Lake as a representative of the silica-saturated (peralkaline granite) class.

Lovozero

The 362 Ma Lovozero complex hosts the largest niobium resource in Russia (29.2 Mt of ore grading 0.15 wt.% Nb_2O_5) and has been mined for this metal and the REE since the early 1940s (Féménias et al., 2005, Pakhomovsky et al., 2014, Kalashnikov et al., 2016, Mikhailova et al., 2019). The complex is the second largest alkaline igneous layered suite in the World after its neighbor, Khibiny, and intrudes Archean gneiss and Devonian basalt. It has been subdivided into two major units, the 2.5 km thick Differentiated Suite and an overlying Eudialyte Suite up to 800 m thick. These units are referred to as Macro Units II and III, respectively (Féménias et al., 2005). There is also a potentially earlier unit (Macro Unit I) comprising tabular bodies in the lower part of the complex that may represent macro-xenoliths or may be part of the Differentiated Suite (Féménias et al., 2005). The Differentiated Suite comprises Lower and Upper zones containing 5-30 m thick rhythmic sequences that grade upwards from urtite (nearly monomineralic nepheline), through foyaite (alkali feldspar-rich nepheline syenite) to lujavrite (aegrine- and alkali feldspar-rich nepheline syenite); urtite is commonly missing in the lower zone (Fig. 8). The Middle zone is composed of lujavrite. Based on textural relationships, alkali feldspar and nepheline are interpreted to have crystallised first, followed by the ferromagnesian minerals, which occur interstitially to them (Féménias et al., 2005, Mikhailova et al., 2019). The overlying Eudialyte Suite cuts the layering of the Differentiated Suite and differs from the latter in containing abundant eudialyte (~ 6 vol.% versus < 1 vol.% in the Differentiated Suite), a much higher proportion of alkali feldspar and thicker layering (up to 100 m thick). The niobium is concentrated in the Differentiated Suite, as the late-crystallizing mineral loparite-(Ce). It occurs mainly in 10-150 cm thick horizons distributed over a vertical interval of ~1100 m, each of which is located in lujavrite immediately below its contact with the overlying urtite in the rhythmic cycles referred to above (Upper and

Lower zones); there is also a horizon in lujavrite in the Middle Zone (Fig. 8). Four of the loparite-rich horizons have been mined historically, but only the two uppermost horizons are currently being exploited.

Nechalacho

The Nechalacho deposit (Canada) is hosted by a recently explored alkaline layered igneous suite > 1 km thick located in a large 2185 Ma alkaline igneous complex comprising plutons ranging in composition from alkaline gabbro to alkaline granite (the Blachford Igneous Complex; Fig. 9a). The Nechalacho deposit, which was explored mainly for the REE (1.5 wt.% REE_2O_3), contains a resource of 109 Mt of ore grading 0.39 wt.% Nb_2O_5. Although two zones of economic mineralization have been recognized (the Upper Zone and the Basal Zone), both of which are in the upper part of the layered suite, the bulk of the mineralization occurs in the higher-grade Basal Zone (Fig. 9b). Lithologically, the layered sequence comprises nepheline syenites with variable proportions of aegirine and sodalite, and, locally, shows evidence of rhythmic layering. In the upper part of the suite, this evidence is obscured by intense hydrothermal alteration that destroyed much of the primary mineralogy, e.g., aegirine was replaced by biotite and magnetite and the principal ore mineral (eudialyte) in the Basal Zone was pseudomorphed by calcite, fluorite, quartz, biotite, zircon, fergusonite-(Y) and other REE minerals (Fig. 10a). Much of the niobium in the Upper Zone is hosted in zircon and in the Basal Zone initially by eudialyte. During hydrothermal alteration, niobium and yttrium were released from zircon and eudialyte to form fergusonite-(Y) (Fig. 10b). Some of the niobium combined with iron to form columbite-(Fe).

Strange Lake

Strange Lake is a NYF pegmatite-hosted deposit that exemplifies a class of deposits associated with peralkaline granitic plutons, in which N, Y and F refer to niobium, yttrium and fluorine, respectively. The pluton is the youngest member of the Nain Plutonic Suite (1240-1460 Ma) of anorthosites, charnockites, and granites that intruded late Archean to early Proterozoic gneisses, and comprises hypersolvus granite, transsolvus granite and a swarm of apical flat-lying pegmatite sheets and subordinate subvertical dykes (Fig. 11b). Evidence of hydrothermal alteration is widespread and is most intense in the pegmatites and the highly evolved transsolvus granite. The pluton was explored recently for its REE potential and a resource containing 20 Mt of ore grading 1.44 wt% REE_2O_3 (50% heavy rare-earth oxides) and 0.34 wt% Nb_2O_5 was identified in the

pegmatites and the adjacent granite (Vasyukova and Williams-Jones, 2018). Niobium concentrations are elevated in all facies of the pluton, ranging from ~450-500 ppm Nb_2O_5 in the hypersolvus and transsolvus granites to over 5,000 ppm Nb_2O_5 in the pegmatites (Vasyukova and Williams-Jones, 2014). Although the pegmatites are highly altered and, thus, the initial magmatic concentration of niobium may have been modified by hydrothermal processes, analyses of melt inclusions indicate that the magma producing the pegmatites contained ~4,000 ppm Nb_2O_5 (Vasyukova and Williams-Jones, 2019). Thus, the bulk rock concentrations of niobium referred to above were not affected significantly by hydrothermal alteration. In all facies of the intrusion, the niobium is present almost exclusively as pyrochlore, although in many cases the pyrochlore is a product of the alteration of elpidite and/or narsarsukite to gittinsite and titanite, respectively (Fig. 12); unaltered elpidite and narsarsukite can contain in excess of 5,000 ppm Nb. The only other mineral that contains significant niobium is arfvedsonite with up to ~500 ppm Nb (Siegel et al., 2017b). The primary pyrochlore is a REE-rich variety (ceriopyrochlore), containing ~17 wt.% REE_2O_3, whereas the secondary pyrochlore is variably enriched in Pb (up to 27 wt.%).

NIOBIUM RESERVOIRS

The concentration of niobium increases from 0.2 and 0.6 ppm in the depleted and primitive mantle, respectively (Palme and O'Neill, 2014), to 6 ppm in the oceanic crust (Klein, 2003) and 5, 10 and 12 ppm in the lower, middle and upper continental crust, respectively (Rudnick and Gao, 2014). Thus, niobium is strongly fractionated into the oceanic and continental crust. Nonetheless, as discussed below, the mantle is the major reservoir for this metal.

PROCESSES CONCENTRATING NIOBIUM

Magmatic processes

Partial melting

From the preceding deposit descriptions, it is evident that all economic or potentially economic deposits are hosted by carbonatites or alkaline igneous rocks. The corresponding magmas for both these suites of rocks originate in the mantle, indicating that the latter is the main reservoir for niobium. As primary carbonatitic magmas are considered to represent ~0.5 % melting of a carbonated mantle (Dalton and Presnall, 1998), a primitive mantle containing 0.6 ppm Nb would yield a carbonatitic magma with a Nb concentration of 120 ppm (Table 2). In contrast, the same

mantle would yield an alkaline silicate magma containing a much lower concentration, e.g., 30 ppm of niobium if it were the product of 2 % of partial melting. Carbonatitic and alkaline magmas, however, are widely considered to be the products of the partial melting of a carbonated mantle, metasomatically enriched in lithophile and high field strength elements (including niobium) and fluxes such as fluorine and H_2O. Although we do not have estimates of the niobium content of this mantle, the niobium content of the carbonatitic magmas produced by its melting can be roughly estimated from the data compiled by Chakhmouradian (2006) for carbonatites interpreted by him to have been derived directly from the mantle. The average niobium content of these primary carbonatites is ~300 ppm, i.e., nearly three times higher than calculated above for a primitive mantle source. Similarly, the niobium content of the alkaline silicate magmas produced by partial melting of a carbonated mantle can be estimated from the niobium content of the most primitive alkaline silicate rocks, the nature of which varies with the pressure (olivine nephelinite at < 3 GPa and olivine melilitite at > 3 GPa). We have estimated the average niobium content of these two rock-types from the GEOROC database (https://georoc.eu/) to be 119 ppm and 94 ppm, respectively, and assume that the average niobium contents for alkaline silicate magmas derived from the partial melting of a HFSE-enriched carbonated mantle is ~100 ppm. From the above estimates of the niobium contents of the carbonatite and average alkaline silicate magma produced by 0.5 and 2 % partial melting of a carbonated HFSE-enriched mantle, respectively, this mantle is predicted to have a niobium content between 1.6 ppm and 2.1 ppm, i.e., roughly three times higher than primitive mantle (Table 2).

Fractional crystallization and liquid immiscibility

As discussed above, partial melting of a metasomatically enriched mantle plays a major role in the concentration of niobium, producing primary carbonatitic magmas containing ~300 ppm Nb and alkaline magmas with ~100 ppm Nb. The magmatic concentration of niobium in the ore deposits, however, is more than an order of magnitude higher, i.e., up to ~1 wt.% Nb for carbonatite-hosted deposits and up to ~0.2 wt.% Nb for deposits hosted by alkaline silicate rocks. This clearly demonstrates that other processes play a major role in the further concentration of niobium. The most important magmatic process for alkaline silicate magmas is fractional crystallization in magma chambers enroute to the site of final magma emplacement. This, however, cannot explain the enrichment of niobium in primary carbonatitic magmas because they do not need to accumulate

in magma chambers (a prerequisite for processes like the gravity settling of minerals) as their low viscosity allows them to move easily through the crust along narrow fractures to their final site of emplacement. Thus, any significant enrichment of carbonatitic magmas in niobium prior to emplacement is unlikely to be due to fractional crystallization.

Fractional crystallization of alkaline silicate magmas

The role of fractional crystallization in concentrating metals like niobium in alkaline igneous systems can be evaluated using the examples of the Nechalacho and Strange Lake REE-Nb deposits. As discussed above, the silicate magmas derived from the partial melting of metasomatically HFSE-enriched mantle have a Nb concentration of ~100 ppm. These magmas evolve by fractional crystallization to produce the magmas that crystallize the intrusions hosting REE-Nb deposits. In the case of Nechalacho, the intrusion is a layered igneous complex composed mainly of aegirine-nepheline syenite. Although the niobium content of the magma at the time of emplacement is not known, it can be roughly estimated from the weighted average niobium content of the different units in the complex, which we have calculated for a 1.1 km vertical hole drilled from the top to near the bottom of the layered suite to be ~350 ppm. Significantly, this concentration is very similar to that of dykes intersected in the complex (by drilling), which are compositionally similar to it. These dykes have an average niobium content of 344 ppm. The Strange Lake deposit is hosted by a peralkaline granite comprising hypersolvus granites, transsolvus granite and pegmatites. The least evolved of these units, which has been interpreted to represent the parental magma, is a hypersolvus granite containing ~300 ppm Nb.

The niobium concentrations estimated for the parental magmas to the Nechalacho and Strange Lake complexes are roughly three times higher than those of the magmas initially produced by partial melting of a metasomatically HFSE-enriched mantle. We interpret this to indicate that these initial magmas underwent fractional crystallization prior to their emplacement in the middle (Nechalacho; Möller and Williams-Jones, 2016) and upper (Strange Lake; Vasyukova et al., 2016) crust. To estimate the degree of this fractional crystallization we employed the fractional crystallization equation of Neumann et al. (1954):

$$C_l/C_o=F^{(D-1)} \quad (1)$$

in which C_o is the initial concentration of the element of interest (Nb) in the magma, C_l is its concentration in the residual liquid after fractionation, F is the fraction of melt remaining after crystallization and D is the mineral/melt partition coefficient. In modeling the fractionation of the initial magma prior to the crystallization of the Nechalacho layered complex, we assumed that the main fractionating phases were olivine and clinopyroxene, that the initial Nb content was 100 ppm and that the value of D for olivine and clinopyroxene is 0.01 (the D value is from Bedard (2005, 2014)). Based on these assumptions, the percentage of fractional crystallization needed to produce the Nechalacho parental magma is 72 % (Table 2). The fractional crystallization path that yielded the parental magma for the Strange Lake pluton is more complex. As discussed by Vasyukova and Williams-Jones (2020), the initial magma evolved by a combination of fractional crystallization and assimilation of lower crustal material to produce a monzonitic magma. This latter magma evolved by further fractional crystallization to produce an A-type granitic magma. Because of the very low concentration of niobium in the lower crust (6 ppm) and the modest degree of assimilation (10 to 15 %; Siegel et al., 2017a), the impact of assimilation was negligible. Using the fractional crystallization model presented above (the fractionating minerals are the same, except for plagioclase for which the D value is even lower), the degree of fractional crystallization would have been 67 % (Table 2).

The REE-Nb ore in the Nechalacho deposit has a concentration of 0.39 wt.% Nb_2O_5, i.e., nearly an order of magnitude higher than that of the putative parental magma. This mineralization is interpreted to represent the end stage of fractional crystallization of the layered suite that proceeded from the bottom up, and less so from the top down, leaving a very small proportion of liquid that crystallized eudialyte, zircon, aegirine and nepheline (Sheard et al., 2012, Möller and Williams-Jones, 2016). Using Equation 1, we modeled this fractional crystallization, assuming a weighted niobium concentration for the Upper Zone, the Basal Zone and intervening nepheline syenite of ~2,200 ppm Nb and a D value for the fractionating minerals (aegirine and nepheline) of 0.01. The estimated degree of fractional crystallization is 84 % (Table 2). Although, as mentioned above, the Upper Zone and Basal Zone experienced intense hydrothermal alteration, a detailed investigation of the ores has shown that there was negligible subsolidus remobilization of the niobium (Timofeev and Williams-Jones, 2015).

The potentially economic niobium (and REE) mineralization of the Strange Lake pluton has a similar grade to the Nechalacho deposit, i.e., 0.3 wt.% Nb_2O_5, and is concentrated in subhorizontal pegmatite pegmatites sheets in the apical parts of the pluton (significantly, melt inclusions in the pegmatites contain roughly the same concentration Nb_2O_5). These pegmatites represent the end stage of fractional crystallization of a parental magma containing ~300 ppm Nb that evolved through hypersolvus and then transsolvus facies of granite. An important feature of the Strange Lake deposit is that a fluoride liquid segregated from the main silicate liquid (Vasyukova and Williams-Jones, 2014, 2016) and thus, in principle, could have complemented fractional crystallization in concentrating the niobium, as was the case for the REE. The concentration of niobium in fluoride melt inclusions, however, is below the detection limit. These findings are consistent with the experimentally determined fluoride-silicate melt partition coefficients reported by Veksler et al. (2012), showing that niobium prefers the silicate melt. Assuming a D value for the fractionating minerals of ≤0.01 (Veksler et al., 2012), the pegmatites hosting the Strange Lake niobium mineralization formed after 86 % fractional crystallization of the corresponding magma (Table 2).

Fractional crystallization of carbonatitic magmas (post-emplacement)

In principle, fractional crystallization could be an important process in concentrating niobium after carbonatitic magma emplacement. The problem, however, is that pyrochlore occurs almost invariably as euhedra to subhedra in carbonatites, suggesting that it is an early formed mineral. Experimental studies, however, have shown that, except for magmas with elevated concentrations of sodium, the solubility of niobium in carbonatitic magmas is extremely high. Indeed, the concentrations of dissolved niobium can reach percentage levels (Jago and Gittins, 1993, Mitchell and Kjarsgaard, 2002a, Mitchell and Kjarsgaard, 2002b). An extremely high degree of fractional crystallization would, therefore, be required to saturate the magma in pyrochlore, for example, assuming an initial niobium content of the magma of 300 ppm and a saturation niobium concentration of 1 wt.%, the degree of fractional crystallization would be ~97 wt.%. If this were the case, pyrochlore would form interstitially to the earlier crystallizing minerals, i.e., it would not occur as euhedra or subhedra. Theoretically, pyrochlore could crystallize early from a sodium-rich carbonatitic magma, accumulate and then be mechanically transported by another carbonatitic magma to the site of emplacement to form an economic deposit. We consider this highly unlikely

for the following reasons: 1) early crystallization of pyrochlore would require its saturation at a concentration of no more than a few hundred ppm of Nb and, thus, the pyrochlore would have to crystallize from a large volume of magma; 2) the pyrochlore would need to accumulate in a magma chamber, the development of which is precluded by the low viscosity of carbonatitic magmas (Vasyukova and Williams-Jones, 2022); and 3) the carbonatitic magma transporting the pyrochlore would be sodium-poor (niobium deposits are hosted by calcite and dolomite carbonatites, see above), and the pyrochlore would dissolve during transport. For the reasons given above, we conclude that fractional crystallization does not play a role in concentrating the niobium of carbonatitic magmas.

The assumption underlying the above discussion of the role of fractional crystallization in concentrating niobium is that carbonatitic magmas are the primary products of partial melting of the mantle. It is possible, however, that carbonatitic magmas form in the crust from extreme fractional crystallization of carbonate-rich alkaline silicate magmas. In principle, this could lead to a secondary carbonate magma enriched in niobium. As the degree of fractional crystallization of the silicate magma required to produce a carbonatitic magma varies inversely with the degree of partial melting, the combined effect of the two processes would lead to a carbonatitic magma with the same niobium content as a primary carbonatitic magma, i.e., ~300 ppm Nb. Thus, irrespective of whether the carbonatitic magma is primary or secondary, fractional crystallization cannot explain the concentration of niobium observed in carbonatite-hosted niobium deposits.

Carbonate-silicate liquid immiscibility

An alternative to fractional crystallization for producing secondary carbonatitic magmas is carbonate-silicate liquid immiscibility. This process, however, is restricted to carbonatitic magmas enriched in Na_2O (Brooker and Kjarsgaard, 2011), whereas we consider the magmas that produce niobium-rich carbonatites to be sodium-poor. Moreover, the partitioning of niobium between such Na_2O-rich magmas and silicate magmas favours the silicate liquid (Veksler et al., 2012). Thus, even if liquid immiscibility were to occur, the resulting carbonatitic magma would be relatively depleted in niobium. We, therefore, conclude that carbonate-silicate liquid immiscibility does not play a role in the formation of carbonatite-hosted niobium deposits.

Carbonatitic magma-mediated metasomatism

In the preceding paragraphs, we have shown that fractional crystallization and liquid immiscibility cannot explain the enrichment of niobium required to form carbonatite-hosted niobium deposits. One of the lines of evidence for this is the euhedral nature of the pyrochlore and its common occurrence as inclusions in other phases, including carbonates, which suggest that it is an early liquidus mineral and is, thus, relatively insoluble in carbonatitic magmas. As discussed above, however, experimental studies have demonstrated that the latter cannot be the case, except for magmas with elevated sodium concentrations. In the paragraphs below, we present a hypothesis involving the interaction of carbonatitic magmas with their host rocks that we believe reconciles the apparent contradiction between textural observations and the results of experiments relating to the solubility of niobium in carbonatitic magmas.

Owing to their extremely low viscosity (similar to that of water), carbonatitic magmas are able to interact with their host rocks in a manner similar to that of hydrothermal fluids, i.e., they are able to penetrate along micro fractures and grain boundaries, and pervasively alter the rocks. Based on this observation, Vasyukova and Williams-Jones (2022) proposed that carbonatitic magmas could alter their host rocks metasomatically and used the hypothesis to explain the various features of carbonatite-phoscorite complexes, including the spatial and temporal association of carbonatites with ultramafic rocks. Here, we employ this hypothesis to resolve the contradictory observations on the solubility of niobium in carbonatitic magmas and explain the formation of economic carbonatite-hosted niobium deposits using the example of the St Honoré carbonatite.

A feature of the St Honoré deposit is the close spatial association of high grade niobium mineralization with phlogopitites that we interpret to be the products of the interaction of a magnesio-carbonatitic magma with K-feldspar-dominated syenites. The interaction led to the metasomatic alteration of the K-feldspar to phlogopite via the reaction:

$$KAlSi_3O_8\,(\text{K-feldspar}) + 3CaMg(CO_3)_2\,(\text{magma}) + H_2O = KMg_3(Si_3Al)O_{10}(OH)_2\,(\text{phlogopite}) + 3CO_2 + 3CaCO_3\,(\text{magma}) \quad (2)$$

This reaction decreased the volume of carbonatitic magma and enriched it in Ca, leading to the crystallization of calcite, because of the displacement of the magma composition to the calcite liquidus (Fig 13). The result was a further reduction in the proportion of residual liquid and a

progressive increase in the concentration of non-carbonate components. Eventually, this concentration was sufficient to saturate the magma in pyrochlore and minerals such as apatite, magnetite and phlogopite, leading to the crystallization of a rock with the composition of phoscorite (nelsonite). Pyrochlore was the first of these minerals on the liquidus, as shown by its euhedral habit and occurrence as inclusions in the other phases. As this phoscoritic magma was the product of carbonatitic magma/syenite interaction (phlogopitization), it commonly accumulated adjacent to the phlogopitized syenite, thereby explaining the association of the phlogopitites with high concentrations of niobium. Much of the phoscoritic magma (liquid or partially crystallised), however, was swept up by subsequent batches of carbonatitic magma to form the apatite-phlogopite-magnetite-pyrochlore lenses and layers that characterize the niobium mineralized "banded" carbonatites of the St Honoré complex. The processes described above are illustrated in Figure 14.

Although the model presented here is based on observations made at St Honoré, it is applicable to many other carbonatite complexes. For example, the phlogopitized ijolites in the Oka carbonatite are noticeably enriched in pyrochlore and, within the carbonatite, the pyrochlore is concentrated in apatite-magnetite-phlogopite-rich layers and lenses. The latter is also true for the Aley and Mt Weld carbonatites. An important feature of both the Araxá and Catalão I complexes is the abundance of phlogopitite and phoscorite (nelsonite). Moreover, at Araxá, the highest concentrations of primary niobium mineralization are associated with phlogopitite and at Catalão I, the bulk of the primary niobium ore is hosted by nelsonite dykes located in a sea of phlogopitic rocks. In summary, the association of the niobium mineralization with phlogopitites and apatite-magnetite-phlogopite-rich rocks (phoscorite/nelsonite) in the World's major niobium deposits provides strong support for the hypothesis that this mineralization owes its origin to carbonatitic magma-host rock metasomatic reactions.

Hydrothermal processes

In many of the complexes hosting niobium deposits there is evidence of widespread hydrothermal alteration and, commonly, the primary Nb-bearing minerals have been altered. For example, the ore zones in the Nechalacho deposits have been so intensely altered by hydrothermal fluids that the primary mineralogy and many of the primary igneous textures have been obliterated (primary aegirine and nepheline were altered to biotite, magnetite and albite; Sheard et al., 2012). In the

Basal Zone, the main niobium-bearing mineral, eudialyte, was pseudomorphed by a variety of minerals including fergusonite-(Y), the principal niobium ore mineral. The restriction of fergusonite to the confines of pseudomorphs after primary eudialyte (Fig. 10a) indicates that niobium was largely immobile during alteration of this mineral. In the Upper Zone, the main primary niobium-bearing mineral, zircon, was replaced by fergusonite-(Y) (Fig. 10b). However, fergusonite-(Y) also occurs separately from but invariably within microns of zircon crystals, indicating that niobium was mobile, albeit on a very small scale (Timofeev and Williams-Jones, 2015). At Strange Lake, two of the main primary Nb-bearing minerals, elpidite and narsarsukite, were pseudomorphed to gittinsite and titanite, respectively, releasing their niobium to form pyrochlore in and adjacent to the pseudomorphs (Fig. 12). This demonstrates that, as in the Nechalacho deposit, niobium was only mobile on a scale of microns. Further support for the relative immobility of niobium is provided by the St Honoré carbonatite, where primary pyrochlore was pseudomorphed by columbite-(Fe) (Fig. 3e and f). A similar observation can be made for the Aley carbonatite, where primary pyrochlore was pseudomorphed by columbite-(Fe) and fersmite (Chakhmouradian et al., 2015). These observations clearly indicate that in most niobium deposits hydrothermal alteration produces secondary niobium minerals but does not mobilize niobium, consistent with experimental and theoretical studies showing that niobium mineral solubility is extremely low (Timofeev et al., 2015), except at conditions rarely present during the hydrothermal alteration of niobium deposits in nature, e.g., very high fluoride activity, very low Ca activity and unusually high temperature (Akinfiev et al., 2020).

Supergene enrichment

To our knowledge, the only niobium deposits that have yielded supergene ores or potential ores are carbonatite-associated. This section, therefore, will be restricted to supergene processes affecting carbonatite-hosted niobium mineralization. The major carbonatite deposits described above, which contain abundant laterite-hosted niobium mineralization, are all characterized by supergene enrichment, except for the Catalão I deposit. Most, and probably all of this enrichment can be attributed to the loss of carbonate during weathering, which would have left a residue of hydrated iron oxides and altered silicate minerals. In the case of Catalão I, however, the primary mineralization is hosted by nelsonites (phoscorites) and, consequently, carbonate loss would have

been minor and would likely have been largely compensated by the formation of hydrous secondary minerals, such as goethite and smectite.

Except for the Seis Lagos deposit, the principal niobium ore mineral in the laterites is pyrochlore. This pyrochlore differs considerably from the primary pyrochlore by containing a high proportion of vacancies and high concentrations of Ba and/or Sr and/or Ce and/or K. In some deposits, this secondary pyrochlore comprises a single compositional variety, for example, at Araxá and Catalão I, the laterite-hosted pyrochlore is bariopyrochlore, in the case of Araxá, reflecting the fact that the carbonatites typically contain 2 to 3 wt.% BaO (Traversa et al., 2001); at Catalão I, the primary pyrochlore evolved to bariopyrochlore. In other deposits, there are two or more secondary pyrochlore varieties. For example, in the Lueshe deposit, the laterite-hosted pyrochlore may be Ba-, Sr-, Ce- and K-rich, depending on location in the laterite profile (Fig. 5). The same is also true for the Mt Weld laterite, except that the K-rich variety is absent. At Seis Lagos, the main ore mineral is niobian rutile. It may also be significant that the Seis Lagos deposit has the highest grade (2.81 wt.% Nb_2O_5, corresponding to an enrichment factor of >3) of any of the deposits considered in this study.

The enrichment of the laterite-hosted pyrochlore in elements like Ba, Sr, Ce and K partly reflects their relative abundance in the primary carbonatite. Mainly, however, it reflects the replacement of the A-site elements, Na and Ca, in the primary pyrochlore during weathering of the carbonatite by meteoric waters, acidified through their interaction with organic matter and neutralized by carbonate minerals (Fig. 15). This replacement is controlled by the pyrochlore structure, which can be envisaged as comprising B-site cations bonded to X-site anions (O^{2-}) to form the $B_2O_6^{2-}$ component (mainly $Nb_2O_6^{2-}$), and A-site cations bonded to Y-site anions to form the A_2Y^{2+} component (commonly, $[Ca^{2+}Na^{+}F^{-}]^{2+}$). These two components are bonded electrostatically to neutralize charge (ionic bonding). Because of the high charge of the cations occupying the B-site, the $B_2O_6^{2-}$ component is very strongly bonded (dominantly, covalent) and therefore, resists alteration, whereas the lower charge of the ions in the A_2Y^{2+} component and the resulting weaker bonding make it much more susceptible to alteration. In the case of a pyrochlore containing the component $[Ca^{2+}Na^{+}F^{-}]^{2+}$, replacement of the cations by K^{+}, Ba^{2+} or Ce^{4+} would proceed via the reactions:

$$[Ca^{2+}Na^{+}F^{-}]^{2+} + 2K^{+} = [2K^{+}\boxed{Y}]^{2+} + Ca^{2+} + Na^{+} + F^{-} \quad (3)$$

$$[Ca^{2+}Na^{+}F^{-}]^{2+} + Ba^{2+} = [Ba^{2+}\boxed{A}\,\boxed{Y}]^{2+} + Ca^{2+} + Na^{+} + F^{-} \quad (4)$$

$$[Ca^{2+}Na^{+}F^{-}]^{2+} + Ce^{4+} = [Ce^{4+}\boxed{A}\,O^{2-}]^{2+} + Ca^{2+} + Na^{+} + F^{-} \quad (5)$$

These replacement reactions are consistent with hard/soft acid/base theory (Pearson, 1963, Williams-Jones and Migdisov, 2014), in which a hard acid bonds preferentially with a hard base and a soft acid with a soft base (HSAB). According to this theory, the $Nb_2O_6^{2-}$ component of the pyrochlore would be a soft base and would, therefore, prefer soft acids. The replacement of the component $[Ca^{2+}Na^{+}F^{-}]^{2+}$ by the components $[2K^{+}, \boxed{Y}]^{2+}$ or $[Ba^{2+}, \boxed{A}, \boxed{Y}]^{2+}$ conforms with HSAB theory in that K^{+} and Ba^{2+} have smaller charge to radius ratios and, therefore, are softer than Na^{+} and Ca^{2+}, respectively. This, taken in conjunction with their vacancies, makes the $[2K^{+}, \boxed{Y}]^{2+}$ or $[Ba^{2+}, \boxed{A}, \boxed{Y}]^{2+}$ components softer than the $[Ca^{2+}Na^{+}F^{-}]^{2+}$ component. More generally, an A_2Y^{2+} component containing Ca^{2+} and/or Na^{+} will be harder than an A_2Y^{2+} component containing Ba^{2+}, Sr^{2+}, K^{+} and Ce^{4+}, thereby explaining the enrichment of elements like Ba, Sr, K and Ce and depletion of Na, Ca and F in the laterite-hosted pyrochlore.

At the onset of laterite development, the acidified meteoric water is rapidly neutralized by the carbonatite and pyrochlore composition evolves mainly by replacement (Stage I, Fig. 15a). With thickening of the laterite, the proportion of carbonate minerals decreases sharply, the neutralization is, therefore, slower and leaching takes over from replacement as the dominant control on pyrochlore composition. In the extreme, with a very thick laterite developed in an equatorial setting, the ongoing weathering may lead to complete leaching of the A- and Y-sites in pyrochlore, leaving behind a Nb_2O_5 skeleton (Stage II, Fig. 15b) produced by the reaction:

$$Nb_2O_6^{2-} + 2H^{+} = Nb_2O_5 + H_2O \quad (6)$$

In summary, during early stages of laterite development, neutralization of the weathering fluid dominates and facilitates the replacement of Na and Ca in the primary pyrochlore by various combinations of Ba, Sr, Ce and K supplied by the dissolution of the carbonatite. If, however, the availability of acidic fluids is prolonged, the continued leaching of the pyrochlore will leave behind nothing more than a skeleton of Nb_2O_5 (Fig. 15).

We attribute the presence of niobian rutile in many laterite ores and its occurrence as the principal ore mineral at Seis Lagos to prolonged intense weathering, the breakdown of titanomagnetite to ferric oxide minerals and rutile, and the reaction of rutile with an aqueous niobium species. According to this hypothesis, the precursor to the aqueous niobium hydroxide species is the Nb_2O_5 skeleton left behind after complete leaching of pyrochlore by the weathering fluids. We propose that the Nb_2O_5 skeleton was relatively unstable (a mineral with the composition of Nb_2O_5 has not been reported) and, therefore, was amenable to hydration and dissolution, forming $Nb(OH)_4^+$ (the dominant niobium hydroxide species at ambient temperature; Peiffert et al., 2010), thereby facilitating reaction of the niobium with rutile to form niobian rutile. Thus, we envisage the formation of niobian rutile to occur in two steps. In the first step, the exsolved ilmenite (or ulvospinel) component of the titanomagnetite breaks down to ferric hydroxides and rutile via the reaction:

$$FeTiO_3 + 0.5H_2O + 0.25O_2 = FeO(OH) + TiO_2 \quad (7)$$

and in the second step, the niobium hydroxide species reacts with the rutile and ferric hydroxide to form niobian rutile via the reaction:

$$0.8TiO_2 + 0.1FeO(OH) + 0.1Nb(OH)_4^+ = Fe_{0.1}Ti_{0.8}Nb_{0.1}O_2 + 0.1H^+ + 0.2H_2O \quad (8)$$

The composition of the niobian rutile was selected to be within the range of niobian rutile compositions reported by Giovannini et al. (2017) for the Seis Lagos laterite. Because of its very low solubility (~9 ppb at 25 oC and a pH 5.5; calculated from Peiffert et al., 2010), niobium is relatively immobile during weathering and, thus, Reaction 8 depends on the availability of rutile proximal to the decomposed pyrochlore (the ferric hydroxide is ubiquitous).

To summarize, weathering of pyrochlore, the principal ore mineral in carbonatite-hosted niobium deposits, proceeds via replacement and leaching of components in the A-site to form laterite ores characterized by pyrochlore with high concentrations of elements like Ba (the case for Araxá and Catalão I). However, in the extreme case exemplified by Seis Lagos, the pyrochlore A-site and Y-site are completely leached, leaving behind a Nb_2O_5 skeleton that reacts locally with the breakdown products of titanomagnetite to form the niobium ore mineral, niobian rutile.

CONCLUSIONS

Niobium is an incompatible element that is present in very small amounts in the mantle. Consequently, the key to its concentration in the Earth's crust and the formation of economic deposits is the very low degree of partial melting of an enriched carbonated mantle. Thus, carbonatites are the main hosts of niobium ore deposits. Some economic and potentially economic deposits, however, are hosted by alkaline silicate rocks, although the grade of the niobium is considerably lower than that of carbonatite-hosted deposits. Whereas fractional crystallization is the most important process in concentrating metals in silicate magmas, this is not true of carbonatitic magmas, in which niobium is extremely soluble. Instead, we conclude that niobium deposits hosted by carbonatite complexes owe their origin to a metasomatic interaction between the carbonatitic magma and its host rocks that alters the latter and consumes a sufficient proportion of the carbonate component to saturate the residual phoscoritic magma in pyrochlore. This explains the close spatial association of the niobium mineralization with rocks like phlogopitites and its concentration in phoscorites (nelsonites) or the apatite-magnetite-phlogopite-rich layers that characterize the mineralized carbonatites. Hydrothermal processes do not concentrate niobium, although they may change the niobium mineralogy, e.g., alter pyrochlore to columbite-(Fe). Weathering, however, may lead to supergene enrichment due to the considerable loss of mass that accompanies the dissolution of the host carbonatite. As a result, high grade laterite-hosted niobium deposits may be generated from lower grade and even uneconomic niobium mineralization. The overarching conclusion of the study is that niobium is the progeny of the mantle, it is concentrated to economic levels by fractional crystallization and high temperature metasomatic magma-rock interaction and, at ambient temperature, it may be further concentrated by laterite-forming supergene processes.

ACKNOWLEDGEMENTS

The research presented in this paper was funded by a Discovery grant from the National Scientific and Engineering Research Council of Canada (NSERC) and benefited from discussions with the geological staff of Niobec^{Nb}, Guillaume Matton, Alexis Gauthier-Ross, Christian Beaulieu and Marc Lavoie, who also facilitated access to the St Honoré carbonatite.

Figure captions

Figure 1. Geological maps of (a) the Araxa carbonatite complex and (b) the Catalao I carbonatite complex modified from Traversa et al. (2001) and Oliveira et al. (2017), respectively.

Figure 2. Geological maps of (a) the St Honore carbonatite complex and (b) the Oka carbonatite complex modified from an unpublished map provided by Niobec[Nb] and Gold (1972), respectively.

Figure 3. Drill core photographs the St Honoré carbonatite showing (a) – fractured syenite that has been partly altered to phlogopite, (b) – brecciated syenite that has been altered to phlogopitite and (c) – carbonatite with alternating dolomite-rich and apatite-magnetite-phlogopite-pyrochlore-rich layers.

Figure 4. Transmitted light photomicrographs and a backscattered electron (BSE) microscope image showing: (a) – pyrochlore crystals in an aggregate of apatite hosted by dolomite carbonatite; (b) – pyrochlore crystals in an aggregate of apatite hosted by calcite carbonatite; (c) – an early zoned U-Ta-Zr-Th enriched pyrochlore crystal overgrown by a rim of calciopyrochlore within an apatite aggregate in dolomite carbonatite; (d) – calciopyrochlore in coarse-grained phlogopitite; (e) and (f) – transmitted light and BSE images of a pyrochlore crystal largely replaced by columbite-(Fe) associated with apatite in a dolomite carbonatite.

Figure 5. Histograms displaying the relative proportions of ceriopyrochlore, natropyrochlore, kaliopyrochlore, strontiopyrochlore, bariopyrochlore and calciopyrochlore as a function of depth and A-site occupancy in laterite from the Lueshe carbonatite modified after Wall et al. (1996).

Figure 6. A vertical cross-section through the Seis Lagos laterite illustrating the different units and the variations in Nb_2O_5 and TiO_2 contents with depth. Modified after Giovannini et al. (2017).

Figure 7. A schematic cross-section through the Mt Weld laterite and overlying sediments showing the concentrations of Na_2O, SrO, CaO and CeO_2 (in wt.%) in pyrochlore at different depths indicated by the letters A to E. The mineralogy of the alumino-silicate (upper) and apatite (lower) is also reported. Based on Lottermoser and England (1988).

Figure 8. (a) – A schematic cross-section through the Lovozero layered complex showing the distribution of the major units, sub-units and loparite horizons; (b) – A schematic cross-section through a cyclic unit of the Upper Differentiated Suite of the Lovozero complex illustrating variations in the distribution of the principal rock-forming minerals, nepheline, K-feldspar and aegirine-augite and rock types. Also shown is the location of a loparite horizon. Adapted from Kalashnikov et al. (2016) and Mikhailova et al. (2019).

Figure 9. (a) – a geological map showing the location of the Nechalacho Layered Suite in the Blatchford Lake complex; 1 – Grace Lake Granite, 2 – Rim Syenite, 3 – Thor Lake Syenite, 4 – Nechalacho Layered Suite, 5 – Caribou Lake Gabbro, 6 – Archean Granite, HM – Hearne Channel and Mad Lake Granite, WL – Whiteman Lake Quartz Syenite. (b) – a vertical cross-section through the Nechalacho Layered Suite showing the locations of the two ore zones (Upper Zone and Basal Zone) and the principal rock units; 1 – Roof Sodalite Syenite, 2 – Pegmatitic Leucosyenite, 3 – Subporphyritic Leucosyenite, 4 – Foyaite, 5 – Upper Zone, 6 –Basal Zone, 6 – Sodalite Foyaite, 7 – Microlayered Aegirine-Nepheline Syenite. Modified from Möller and Williams-Jones (2016).

Figure 10. (a) – pseudomorphs of eudialyte containing fergusonite-(Y) and zircon in the Basal Zone; (b) – a crystal of zircon partially replaced by fergusonite-(Y) in the Upper Zone. Fg – fergusonite-(Y), Zc – zircon. Modified from Möller and Williams-Jones (2017).

Figure 11. (a) – a geological map of the Strange Lake pluton modified from Vasyukova and Williams-Jones (2018) and (b) – a cross-section through the B-Zone pegmatites (indicated by the line A-B in (a)) modified from Gysi et al. (2016).

Figure 12. (a) - pseudomorphs of gittinsite (medium grey) and quartz (dark grey) after elpidite accompanied by crystals of pyrochlore (white) in a matrix of quartz. (b) - a pseudomorph of gittinsite and quartz with two associated crystals of pyrochlore and a pseudomorph (outlined by the green dashes) of titanite (medium grey) and quartz after narsarsukite containing several crystals of pyrochlore.

Figure 13. A schematic phase diagram showing relationships among liquid, calcite, dolomite and periclase in the system CaO-MgO-CO_2 as a function of temperature and the mole fraction of $MgCO_3$. The blue arrow indicates the displacement of the liquid composition to the calcite liquidus. See the main text for further detail. L – liquid, Cc – calcite, Dol – dolomite, Per – periclase and S – solid.

Figure 14. A cartoon illustrating the progressive interaction of a carbonatitic magma (dolomitic) with a syenite. (a) – the emplacement of the carbonatitic magma along fractures in K-feldspar-rich syenite; (b) – the alteration of K-feldspar by the carbonatitic magma to phlogopite (green), calcio-carbonatitic magma (medium blue) and CO_2 (bubbles); (c) – crystallization of calcite (dark grey)

from the calcio-carbonatitic magma leaving a residual phoscoritic magma (dark blue) and (d) – incorporation of the residual phoscoritic magma as layers (dark blue) in a later batch of carbonatitic magma (light blue). See the main text for further detail.

Figure 15. A two-stage cartoon showing the alteration of pyrochlore during weathering of carbonatite by mildly acidic meteoric water. (a) – Stage I, illustrating the dissolution of the carbonatite by early aliquots of the meteoric water, the release of Ba^{2+}, K^{+}, Sr^{2+} and Ce^{4+} to the neutralized water and the replacement of Na^{+} and Ca^{2+} in the pyrochlore by these cations; (b) – Stage II, illustrating that in the absence of carbonatite (dissolved), further aliquots of meteoric water remain acidic and leach the A-site cations to yield a skeleton of Nb_2O_5. See the main text for further detail.

Acknowledgements

The research presented in this paper was funded by a Discovery grant from the National Scientific and Engineering Research Council of Canada (NSERC).

References

Akinfiev, N. N., Korzhinskaya, V. S., Kotova, N. P., Redkin, A. F., and Zotov, A. V., 2020, Niobium and tantalum in hydrothermal fluids: Thermodynamic description of hydroxide and hydroxofluoride complexes: Geochimica et Cosmochimica Acta, v. 280, p. 102-115.

Atencio, D., Andrade, M. B., Christy, A. G., Gieré, R., and Kartashov, P. M., 2010, The pyrochlore supergroup of minerals: nomenclature: The Canadian Mineralogist, v. 48, p. 673-698.

Bedard, J. H., 2005, Partitioning coefficients between olivine and silicate melts: Lithos, v. 83, p. 394-419.

Bedard, J. H., 2014, Parameterizations of calcic clinopyroxene - melt trace element partition coefficients: Geochemistry Geophysics Geosystems, v. 15, p. 303-336.

Berger, V. I., Singer, D. A., and Orris, G. J., 2009, Carbonatites of the World, Explored Deposits of Nb and REE--database and Grade and Tonnage Models, U.S. Geological Survey Open-File Report 2009-1139, 17 p. and database.

Brooker, R. A., and Kjarsgaard, B. A., 2011, Silicate-carbonate liquid immiscibility and phase relations in the system SiO_2-Na_2O-Al_2O_3-CaO-CO_2 at 0.1-2.5 GPa with applications to carbonatite genesis: Journal of Petrology, v. 52, p. 1281-1305.

Chakhmouradian, A. R., 2006, High-field-strength elements in carbonatitic rocks: geochemistry, crystal chemistry and significance for constraining the sources of carbonatites: Chemical Geology, v. 235, p. 138-160.

Chakhmouradian, A. R., Reguir, E. P., Kressall, R. D., Crozier, J., Pisiak, L. K., Sidhu, R., and Yang, P., 2015, Carbonatite-hosted niobium deposit at Aley, northern British Columbia (Canada): Mineralogy, geochemistry and petrogenesis: Ore Geology Reviews, v. 64, p. 642-666.

Cordeiro, P. F., Brod, J. A., Dantas, E. L., and Barbosa, E. S., 2010, Mineral chemistry, isotope geochemistry and petrogenesis of niobium-rich rocks from the Catalão I carbonatite-phoscorite complex, Central Brazil: Lithos, v. 118, p. 223-237.

Cordeiro, P. F. d. O., Brod, J. A., Palmieri, M., de Oliveira, C. G., Barbosa, E. S. R., Santos, R. V., Gaspar, J. C., and Assis, L. C., 2011, The Catalão I niobium deposit, central Brazil: Resources, geology and pyrochlore chemistry: Ore Geology Reviews, v. 41, p. 112-121.

Dalton, J. A., and Presnall, D. C., 1998, The continuum of primary carbonatitic–kimberlitic melt compositions in equilibrium with lherzolite: data from the system CaO–MgO–Al2O3–SiO2–CO2 at 6 GPa: Journal of Petrology, v. 39, p. 1953-1964.

Ekeberg, A., 1803, LVII. Extract from a memoir on the properties of yttria earth compared with those of glucine; on the fossils in which the former of these earths is contained; and on the discovery of a new substance of a metallic nature: The Philosophical Magazine, v. 14, p. 346-350.

Féménias, O., Coussaert, N., Brassinnes, S., and Demaiffe, D., 2005, Emplacement processes and cooling history of layered cyclic unit II-7 from the Lovozero alkaline massif (Kola Peninsula, Russia): Lithos, v. 83, p. 371-393.

Gibson, S. A., Thompson, R. N., Leonardos, O. H., Dickin, A. P., and Mitchell, J. G., 1995, The Late Cretaceous Impact of the Trindade Mantle Plume: Evidence from Large-volume, Mafic, Potassic Magmatism in SE Brazil: Journal of Petrology, v. 36, p. 189-229.

Giovannini, A. L., 2013, Contribuição à geologia e geoquímica do carbonatito e da jazida (Nb, ETR) de Seis Lagos (Amazonas).

Giovannini, A. L., Neto, A. C. B., Porto, C. G., Pereira, V. P., Takehara, L., Barbanson, L., and Bastos, P. H., 2017, Mineralogy and geochemistry of laterites from the Morro dos Seis Lagos Nb (Ti, REE) deposit (Amazonas, Brazil): Ore Geology Reviews, v. 88, p. 461-480.

Gold, D. P., 1963, The relationship between the limestones and the alkaline igneous rocks of Oka and St.-Hilaire, Quebec.

Gold, D. P., 1972, The Monteregian Hills: ultra-alkaline rocks and the Oka carbonatite complex, 1972.

Guarino, V., Wu, F.-Y., Melluso, L., de Barros Gomes, C., Tassinari, C. C. G., Ruberti, E., and Brilli, M., 2017, U–Pb ages, geochemistry, C–O–Nd–Sr–Hf isotopes and petrogenesis of the Catalão II carbonatitic complex (Alto Paranaíba Igneous Province, Brazil): implications for regional-scale heterogeneities in the Brazilian carbonatite associations: International Journal of Earth Sciences, v. 106, p. 1963-1989.

Gysi, A. P., Williams-Jones, A. E., and Collins, P., 2016, Lithogeochemical vectors for hydrothermal processes in the Strange Lake peralkaline granitic REE-Zr-Nb deposit: Economic Geology, v. 111, p. 1241-1276.

Hatchett, C., 1802, III. An analysis of a mineral substance from North America, containing a metal bitberto unknown: Philosophical Transactions of the Royal Society of London, p. 49-66.

Issa Filho, A., Riffel, B., and Sousa, C. A., 2002a, Some aspects of the mineralogy of CBMM niobium deposit and mining and pyrochlore ore processing - Araxá, MG – Brazil: International Symposium Niobium 2001, 2002a.

Issa Filho, A., Riffel, B. F., and Sousa, C. A., 2002b, Some aspects of the mineralogy of CBMM niobium deposit and mining and pyrochlore ore processing - Araxá, MG – Brazil, International Symposium Niobium 2001.

Jago, B., and Gittins, J., 1993, Pyrochlore crystallization in carbonatites: the role of fluorine: South African Journal of Geology, v. 96, p. 149-160.

Kalashnikov, A., Konopleva, N., Pakhomovsky, Y. A., and Ivanyuk, G. Y., 2016, Rare earth deposits of the Murmansk region, Russia—a review: Economic Geology, v. 111, p. 1529-1559.

Kauffman, G. B., 1975, Christian Wilhelm Blomstrand (1826–1897) Swedish chemist and mineralogist: Annals of Science, v. 32, p. 13-37.

Klein, E. M., 2003, Geochemistry of the igneous oceanic crust., *in* Rudnick, R. L., ed., Treatise on Geochemistry, 3: Oxford, Elsevier.

Kovalenko, V. I., Tsaryeva, G. M., Goreglyad, A. V., Yarmolyuk, V. V., Troitsky, V. A., Hervig, R. L., and Farmer, G. L., 1995, The Peralkaline granite-related Khaldzan-Buregtey rare-metal (Zr, Nb, Ree) deposit, Western Mongolia: Economic Geology and the Bulletin of the Society of Economic Geologists, v. 90, p. 530-547.

Lottermoser, B., 1990, Rare-earth element mineralisation within the Mt. Weld carbonatite laterite, Western Australia: Lithos, v. 24, p. 151-167.

Lottermoser, B., and England, B., 1988, Compositional variation in pyrochlores from the Mt Weld carbonatite laterite, Western Australia: Mineralogy and Petrology, v. 38, p. 37-51.

Maravic, H., Morteani, G., and Roethe, G., 1989, The cancrinite-syenite/carbonatite complex of Lueshe, Kivu/NE-Zaire: petrographic and geochemical studies and its economic significance: Journal of African Earth Sciences (and the Middle East), v. 9, p. 341-355.

McCausland, P. J., Pisarevsky, S., Jourdan, F., and Higgins, M., 2009, Laurentia at 571 Ma: Preliminary paleomagnetism and Ar-Ar age of the Ediacaran St Honore alkaliintrusion, Quebec: AGU spring meeting, 2009.

Middlemost, E., 1990, Mineralogy and petrology of the rauhaugites of the Mt Weld carbonatite complex of Western Australia: Mineralogy and Petrology, v. 41, p. 145-161.

Mikhailova, J. A., Ivanyuk, G. Y., Kalashnikov, A. O., Pakhomovsky, Y. A., Bazai, A. V., and Yakovenchuk, V. N., 2019, Petrogenesis of the eudialyte complex of the Lovozero alkaline massif (Kola Peninsula, Russia): Minerals, v. 9, p. 581.

Mitchell, R. H., and Kjarsgaard, B. A., 2002a, Solubility of niobium in the system CaCO3-Ca(OH)(2)-NaNbO3 at 0.1 GPa pressure: Contributions to Mineralogy and Petrology, v. 144, p. 93-97.

Mitchell, R. H., and Kjarsgaard, B. A., 2002b, Solubility of niobium in the system CaCO3–Ca (OH) 2–NaNbO3 at 0.1 GPa pressure: Contributions to Mineralogy and Petrology, v. 144, p. 93-97.

Möller, V., and Williams-Jones, A. E., 2016, Petrogenesis of the Nechalacho Layered Suite, Canada: magmatic evolution of a REE–Nb-rich nepheline syenite intrusion: Journal of Petrology, v. 57, p. 229-276.

Möller, V., and Williams-Jones, A. E., 2017, Magmatic and hydrothermal controls on the mineralogy of the basal zone, Nechalacho REE-Nb-Zr deposit, Canada: Economic Geology, v. 112, p. 1823-1856.

Neumann, H., Mead, J., and Vitaliano, C., 1954, Trace element variation during fractional crystallization as calculated from the distribution law: Geochimica et Cosmochimica Acta, v. 6, p. 90-99.

Oliveira, Í. L., Brod, J. A., Cordeiro, P. F., Dantas, E. L., and Mancini, L. H., 2017, Insights into the late-stage differentiation processes of the Catalão I carbonatite complex in Brazil: New Sr–Nd and C–O isotopic data in minerals from niobium ores: Lithos, v. 274, p. 214-224.

Pakhomovsky, Y. A., Ivanyuk, G. Y., and Yakovenchuk, V., 2014, Loparite-(Ce) in rocks of the Lovozero layered complex at Mt. Karnasurt and Mt. Kedykvyrpakhk: Geology of Ore Deposits, v. 56, p. 685-698.

Palme, H., and O'Neill, H. S., 2014, Cosmochemical estimates of mantle composition, *in* Rudnick, R. L., ed., Treatise on Geochemistry, 3: Oxford, Elsevier.

Pearson, R. G., 1963, Hard and soft acids and bases: Journal of the American Chemical Society, v. 85, p. 3533-3539.

Peiffert, C., Nguyen-Trung, C., Palmer, D., Laval, J.-P., and Giffaut, E., 2010, Solubility of B-Nb2O5 and the hydrolysis of niobium (V) in aqueous solution as a function of temperature and ionic strength: Journal of solution chemistry, v. 39, p. 197-218.

Rachidi, N. R., Nwaila, G. T., Zhang, S. E., Bourdeau, J. E., and Ghorbani, Y., 2021, Assessing cobalt supply sustainability through production forecasting and implications for green energy policies: Resources Policy, v. 74, p. 102423.

Rose, H., 1844, Ueber die Zusammensetzung der Tantalite und ein im Tantalite von Baiern enthaltenes neues Metall: Annalen der Physik, v. 139, p. 317-341.

Rudnick, R. L., and Gao, S., 2014, Composition of the continental crust., *in* Turekian, K. K., and Holland, H. D., eds., Treatise on Geochemistry, 4: Oxford, Elsevier, p. 1-51.

Schulz, K., Piatak, N. M., and Papp, J. E., 2017, Critical Mineral Resources of the United States—Economic and Environmental Geology and Prospects for Future Supply, *in* Klaus J. Schulz, J. H. D., Jr., Robert R. Seal II, and Dwight C. Bradley, ed., Niobium and Tantalum: U.S. Geological Survey, Reston, Virginia.

Sheard, E. R., Williams-Jones, A. E., Heiligmann, M., Pederson, C., and Trueman, D. L., 2012, Controls on the concentration of zirconium, niobium, and the rare earth elements in the Thor Lake rare metal deposit, Northwest Territories, Canada: Economic Geology, v. 107, p. 81-104.

Siegel, K., Williams-Jones, A. E., and Stevenson, R., 2017a, A Nd- and O-isotope study of the REE-rich peralkaline Strange Lake granite: implications for Mesoproterozoic A-type magmatism in the Core Zone (NE-Canada): Contributions to Mineralogy and Petrology, v. 172.

Siegel, K., Williams-Jones, A. E., and van Hinsberg, V. J., 2017b, The amphiboles of the REE-rich A-type peralkaline Strange Lake pluton – fingerprints of magma evolution: Lithos, v. 288, p. 156-174.

Smith, M., Campbell, L., and Kynicky, J., 2015, A review of the genesis of the world class Bayan Obo Fe–REE–Nb deposits, Inner Mongolia, China: Multistage processes and outstanding questions: Ore Geology Reviews, v. 64, p. 459-476.

Smith, M., and Spratt, J., 2012, The chemistry of niobium mineralisation at Bayan Obo, Inner Mongolia, China: constraints on the hydrothermal precipitation and alteration of Nb-minerals: Acta Geol Sinic, v. 86.

Smith, M. P., and Henderson, P., 2000, Preliminary fluid inclusion constraints on fluid evolution in the Bayan Obo Fe-REE-Nb deposit, Inner Mongolia, China: Economic Geology and the Bulletin of the Society of Economic Geologists, v. 95, p. 1371-1388.

Timofeev, A., Migdisov, A. A., and Williams-Jones, A. E., 2015, An experimental study of the solubility and speciation of niobium in fluoride-bearing aqueous solutions at elevated temperature: Geochimica et Cosmochimica Acta, v. 158, p. 103-111.

Timofeev, A., and Williams-Jones, A., 2015, The origin of niobium and tantalum mineralization in the Nechalacho REE Deposit, NWT, Canada: Economic Geology, v. 110, p. 1719-1735.

Traversa, G., Gomes, C. B., Brotzu, O., Buraglini, N., Morbidelli, L., Principato, M. S., Ronca, S., and Ruberti, E., 2001, Petrography and mineral chemistry of carbonatites and mica-rich rocks from the Araxá complex (Alto Paranaíba Province, Brazil): Anais da Academia Brasileira de Ciências, v. 73, p. 71-98.

Tremblay, J., Bédard, L. P., and Matton, G., 2017, Columbitization of fluorcalciopyrochlore by hydrothermalism at the Saint-Honoré alkaline complex, Québec (Canada): New insights on halite in carbonatites: Ore Geology Reviews, v. 91, p. 695-707.

Vallieres, D., Pelletier, P., Gaultier, P., Ferlatte, G., Tremblay, J.-F., and Sirois, R., 2013, NI 43-101 Technical Report, Update on Niobec Expansion, December 2013.

Vasyukova, O. V., and Williams-Jones, A. E., 2014, Fluoride–silicate melt immiscibility and its role in REE ore formation: Evidence from the Strange Lake rare metal deposit, Quebec-Labrador, Canada: Geochimica et Cosmochimica Acta, v. 139, p. 110-130.

Vasyukova, O. V., and Williams-Jones, A. E., 2016, The evolution of immiscible silicate and fluoride melts: Implications for REE ore-genesis: Geochimica et Cosmochimica Acta, v. 172, p. 205-224.

Vasyukova, O. V., and Williams-Jones, A. E., 2018, Direct measurement of metal concentrations in fluid inclusions, a tale of hydrothermal alteration and REE ore formation from Strange Lake, Canada: Chemical Geology, v. 483, p. 385-396.

Vasyukova, O. V., and Williams-Jones, A. E., 2019, Tracing the evolution of a fertile REE granite by modelling amphibole-melt partitioning, the Strange Lake story: Chemical Geology, v. 514, p. 79-89.

Vasyukova, O. V., and Williams-Jones, A. E., 2022, Carbonatite metasomatism, the key to unlocking the carbonatite-phoscorite-ultramafic rock paradox: Chemical Geology, v. 602, p. 120888.

Vasyukova, O. V., Williams-Jones, A. E., and Blamey, N. J. F., 2016, Fluid evolution in the Strange Lake granitic pluton, Canada: Implications for HFSE mobilisation: Chemical Geology, v. 444, p. 83-100.

Veksler, I. V., Dorfman, A. M., Dulski, P., Kamenetsky, V. S., Danyushevsky, L. V., Jeffries, T., and Dingwell, D. B., 2012, Partitioning of elements between silicate melt and immiscible fluoride, chloride, carbonate, phosphate and sulfate melts, with implications to the origin of natrocarbonatite: Geochimica et Cosmochimica Acta, v. 79, p. 20-40.

Wall, F., Williams, C., Woolley, A., and Nasraoui, M., 1996, Pyrochlore from weathered carbonatite at Lueshe, Zaire: Mineralogical Magazine, v. 60, p. 731-750.

Williams-Jones, A. E., and Migdisov, A. A., 2014, Experimental constraints on the transport and deposition of metals in ore-forming hydrothermal systems: Building Exploration Capability for the 21st Century, p. 77-95.

Wollaston, W. H., 1809, XV. On the identity of Columbium and Tantalum: Philosophical Transactions of the Royal Society of London, p. 246-252.

Yang, W. B., Niu, H. C., Shan, Q., Sun, W. D., Zhang, H., Li, N. B., Jiang, Y. H., and Yu, X. A., 2014, Geochemistry of magmatic and hydrothermal zircon from the highly evolved Baerzhe alkaline granite: implications for Zr-REE-Nb mineralization: Mineralium Deposita, v. 49, p. 451-470.

Yelland, G., 2016, Assessment Report on the Technical Work Performed on the Aley Niobium Property in 2014, p. 1-344.

Zurevinski, S. E., and Mitchell, R. H., 2004, Extreme compositional variation of pyrochlore-group minerals at the Oka carbonatite complex, Quebec: evidence of magma mixing?: The Canadian Mineralogist, v. 42, p. 1159-1168.

Williams-Jones, A. E., and Vasyukova, O. V., 2022,
Niobium, Critical Metal and Progeny of the Mantle: Economic Geology, v. doi:10.5382/econgeo.4994.

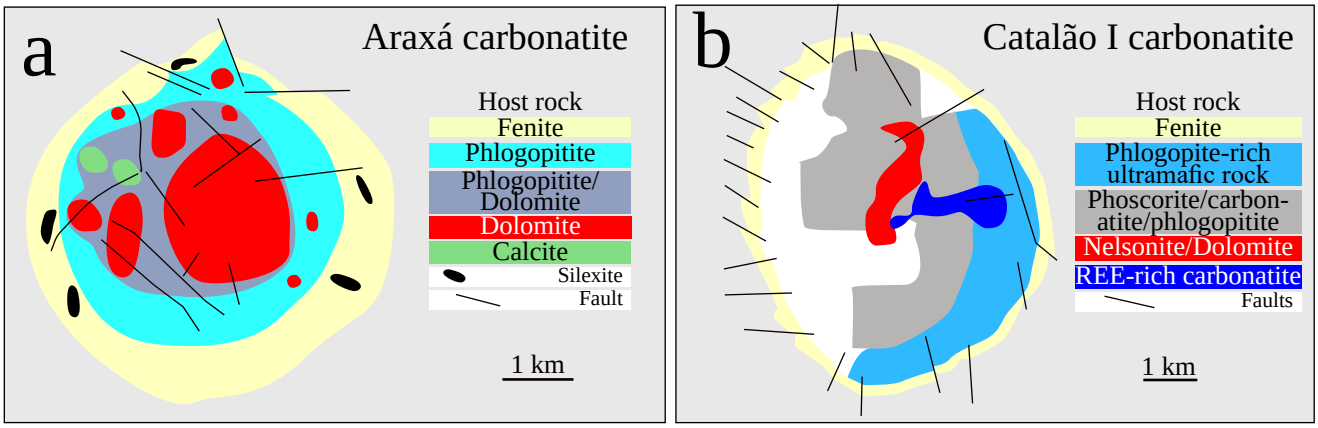

Figure 1 Geological maps of (a) the Araxa carbonatite complex and (b) the Catalao I carbonatite complex modified from Traversa et al. (2001) and Oliveira et al. (2017), respectively.

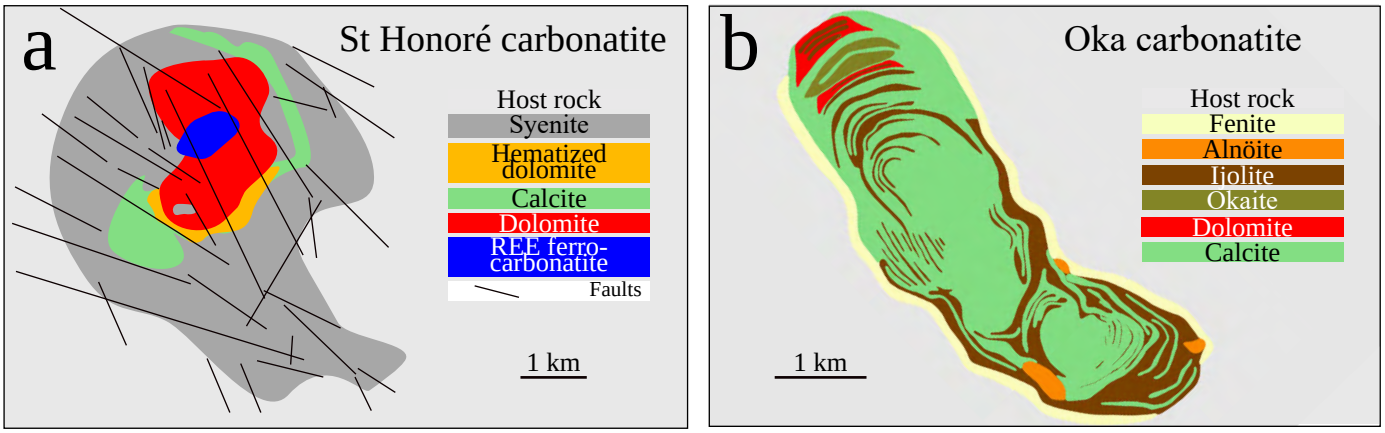

Figure 2 Geological maps of (a) the St Honore carbonatite complex and (b) the Oka carbonatite complex modified from an unpublished map provided by Niobec^{Nb} and Gold (1972), respectively.

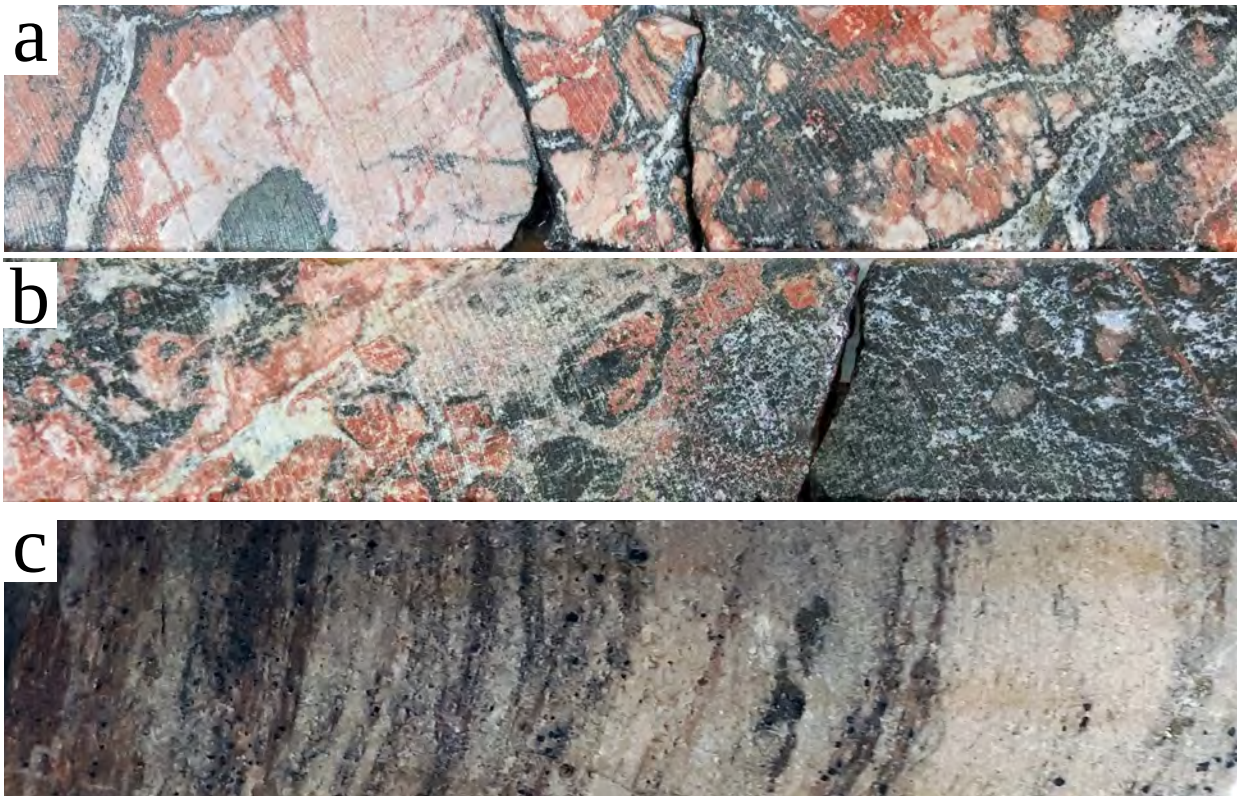

Figure 3 Drill core photographs the St Honoré carbonatite showing (a) – fractured syenite that has been partly altered to phlogopite, (b) – brecciated syenite that has been altered to phlogopitite and (c) – carbonatite with alternating dolomite-rich and apatite-magnetite-phlogopite-pyrochlore-rich layers.

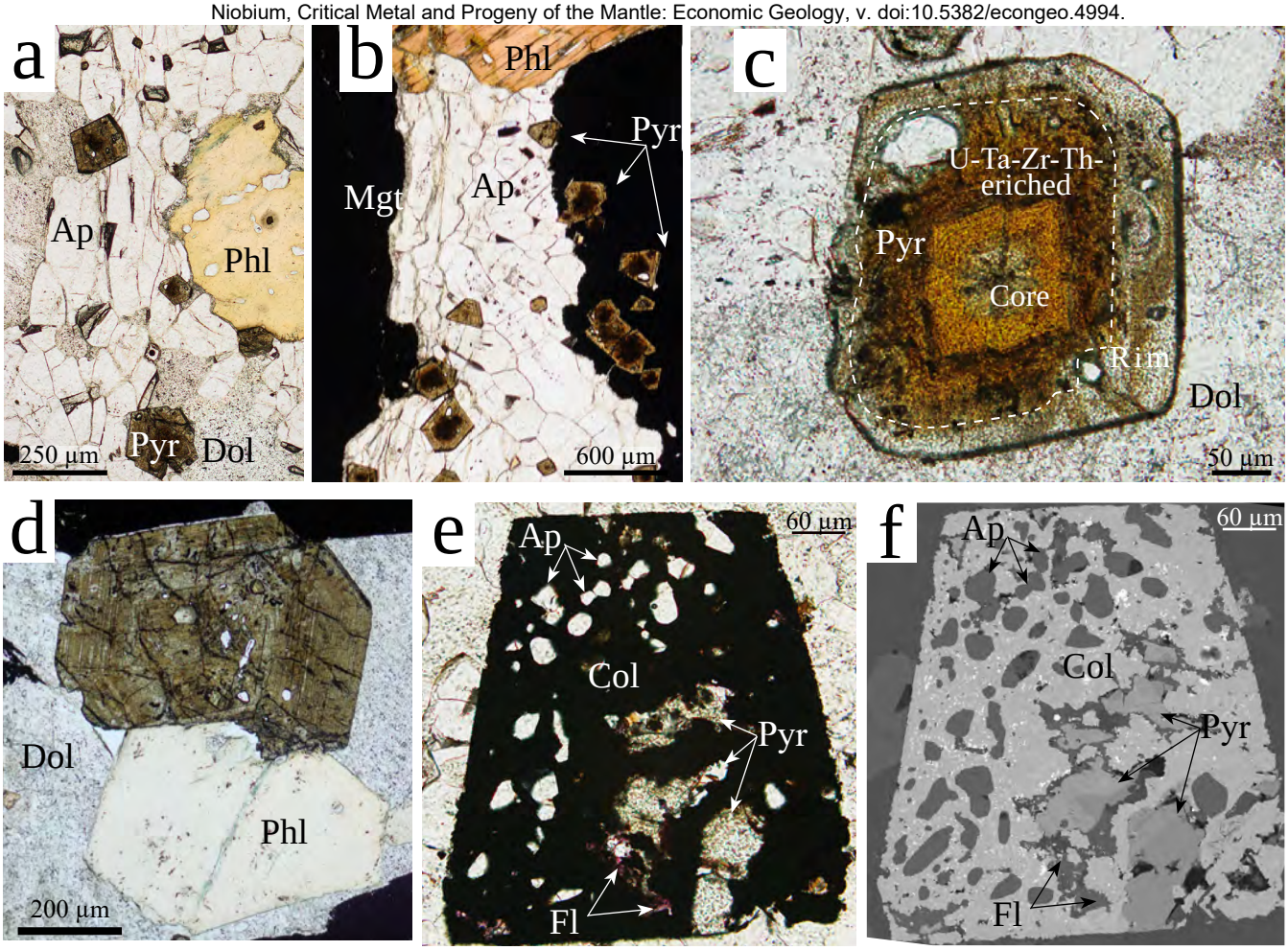

Figure 4 Transmitted light photomicrographs and a backscattered electron (BSE) microscope image showing: (a) – pyrochlore crystals in an aggregate of apatite hosted by dolomite carbonatite; (b) – pyrochlore crystals in an aggregate of apatite hosted by calcite carbonatite; (c) – an early zoned U-Ta-Zr-Th enriched pyrochlore crystal overgrown by a rim of calciopyrochlore within an apatite aggregate in dolomite carbonatite; (d) – calciopyrochlore in coarse-grained phlogopitite; (e) and (f) – transmitted light and BSE images of a pyrochlore crystal largely replaced by columbite-(Fe) associated with apatite in a dolomite carbonatite.

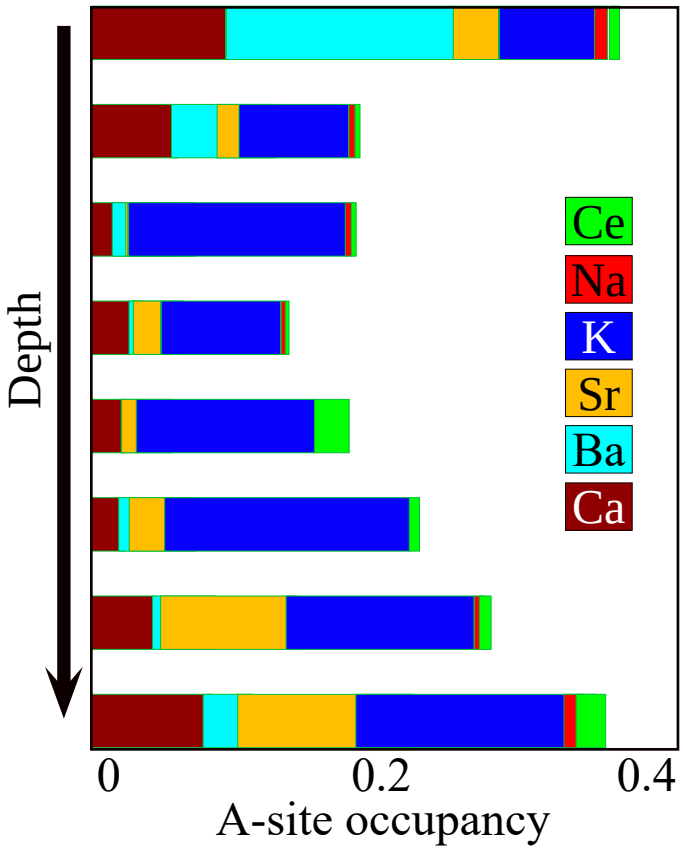

Figure 5 Histograms displaying the relative proportions of ceriopyrochlore, natropyrochlore, kaliopyrochlore, strontiopyrochlore, bariopyrochlore and calciopyrochlore as a function of depth and A-site occupancy in laterite from the Lueshe carbonatite modified after Wall et al. (1996)

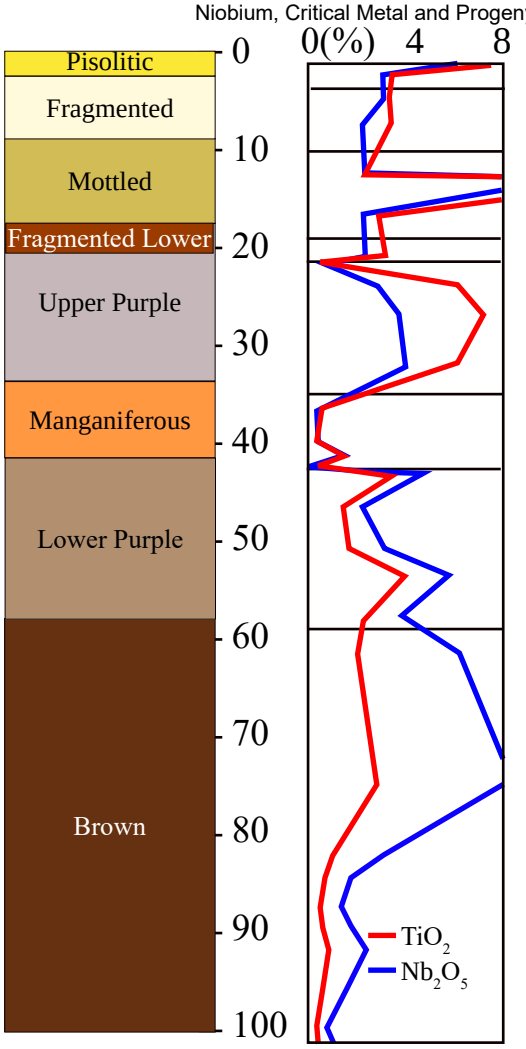

Figure 6 A vertical cross-section through the Seis Lagos laterite illustrating the different units and the variations in Nb_2O_5 and TiO_2 contents with depth. Modified after Giovannini et al. (2017).

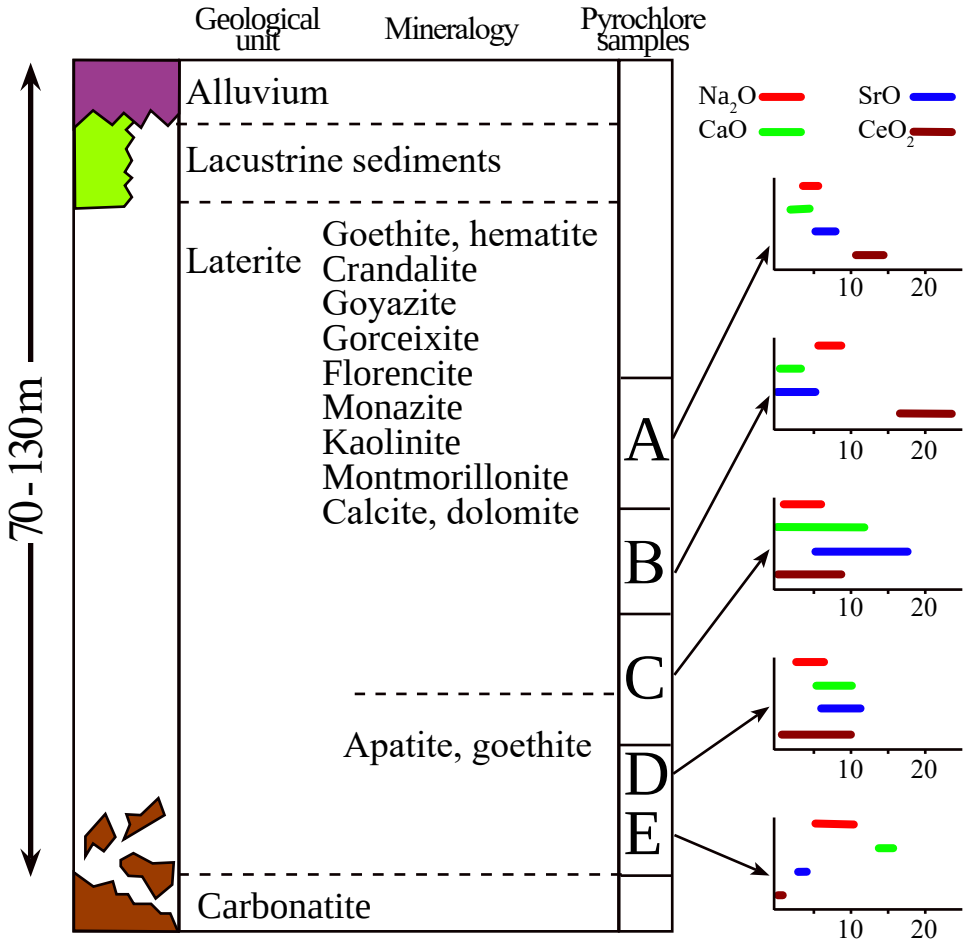

Figure 7 A schematic cross-section through the Mt Weld laterite and overlying sediments showing the concentrations of Na_2O, SrO, CaO and CeO_2 (in wt.%) in pyrochlore at different depths indicated by the letters A to E. The mineralogy of the alumino-silicate (upper) and apatite (lower) is also reported. Based on Lottermoser and England (1988).

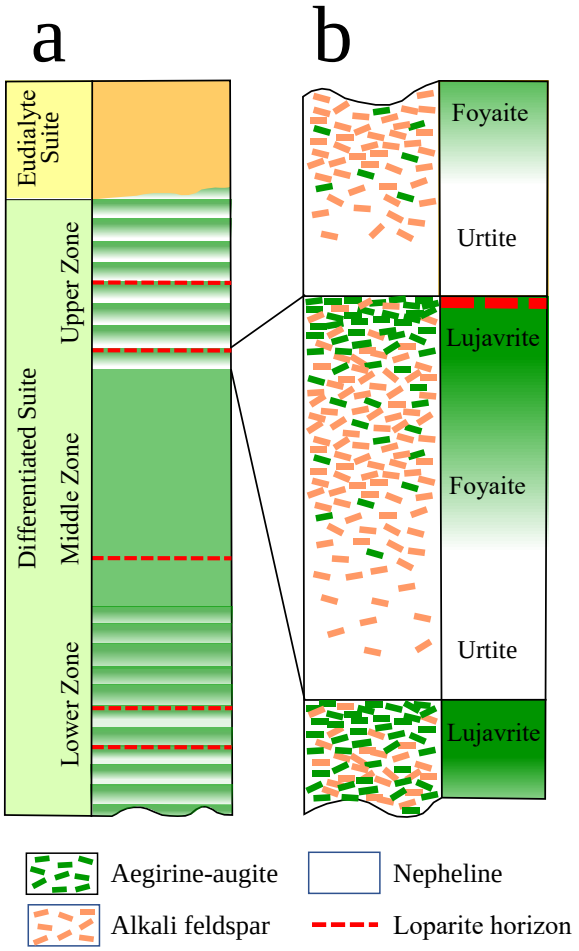

Figure 8 (a) – A schematic cross-section through the Lovozero layered complex showing the distribution of the major units, sub-units and loparite horizons; (b) – A schematic cross-section through a cyclic unit of the Upper Differentiated Suite of the Lovozero complex illustrating variations in the distribution of the principal rock-forming minerals, nepheline, K-feldspar and aegirine-augite and rock types. Also shown is the location of a loparite horizon. Adapted from Kalashnikov et al. (2016) and Mikhailova et al. (2019).

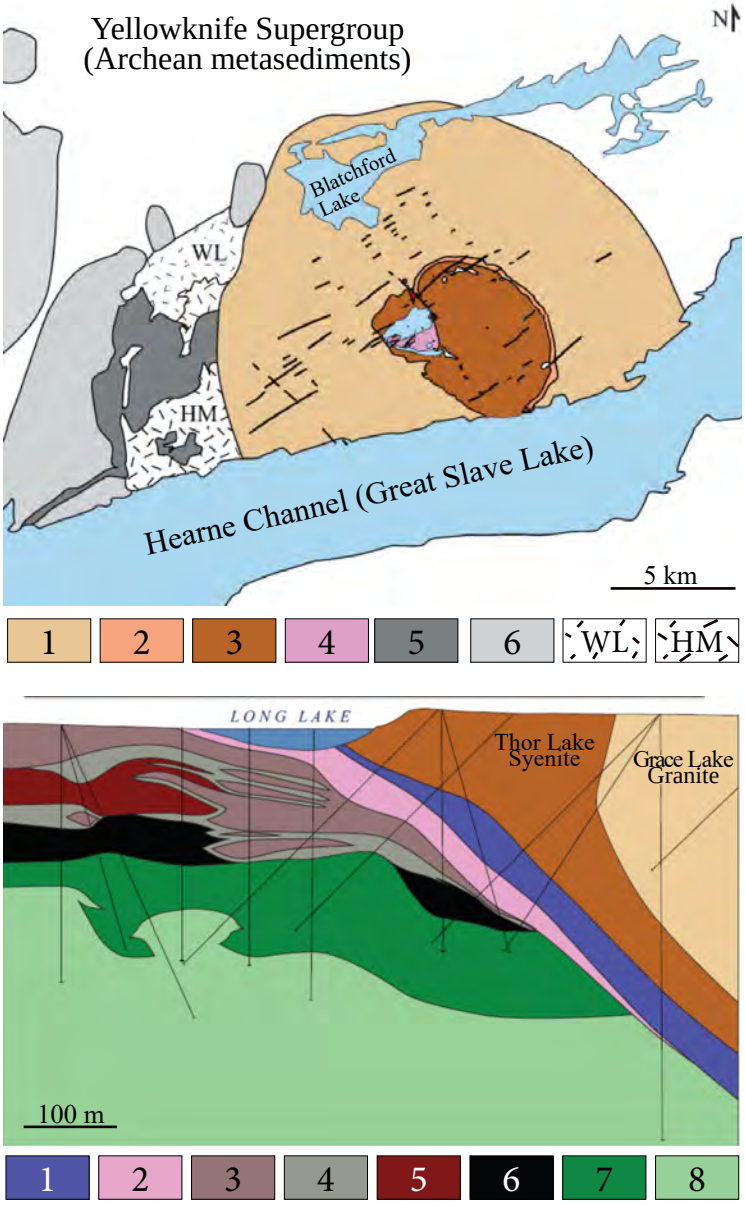

Figure 9 (a) – a geological map showing the location of the Nechalacho Layered Suite in the Blatchford Lake complex; 1 – Grace Lake Granite, 2 – Rim Syenite, 3 – Thor Lake Syenite, 4 – Nechalacho Layered Suite, 5 – Caribou Lake Gabbro, 6 – Archean Granite, HM – Hearne Channel and Mad Lake Granite, WL – Whiteman Lake Quartz Syenite. (b) – a vertical cross-section through the Nechalacho Layered Suite showing the locations of the two ore zones (Upper Zone and Basal Zone) and the principal rock units; 1 – Roof Sodalite Syenite, 2 – Pegmatitic Leucosyenite, 3 – Subporphyritic Leucosyenite, 4 – Foyaite, 5 – Upper Zone, 6 –Basal Zone, 6 – Sodalite Foyaite, 7 – Microlayered Aegirine-Nepheline Syenite.

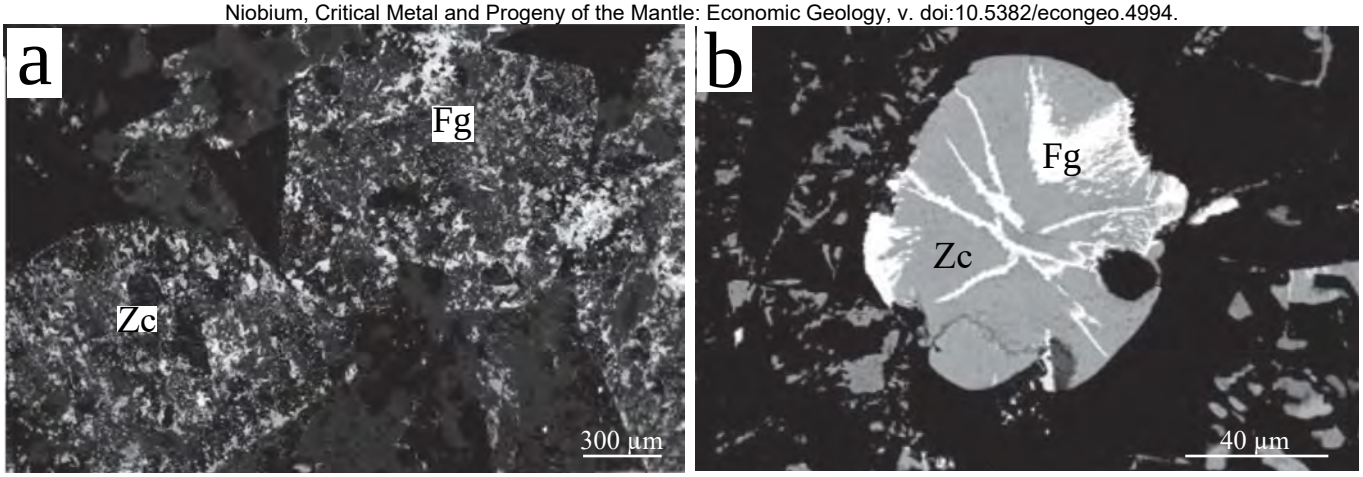

Figure 10 (a) – pseudomorphs of eudialyte containing fergusonite-(Y) and zircon in the Basal Zone; (b) – a crystal of zircon partially replaced by fergusonite-(Y) in the Upper Zone. Fg – fergusonite-(Y), Zc – zircon. Modified from Möller and Williams-Jones (2017).

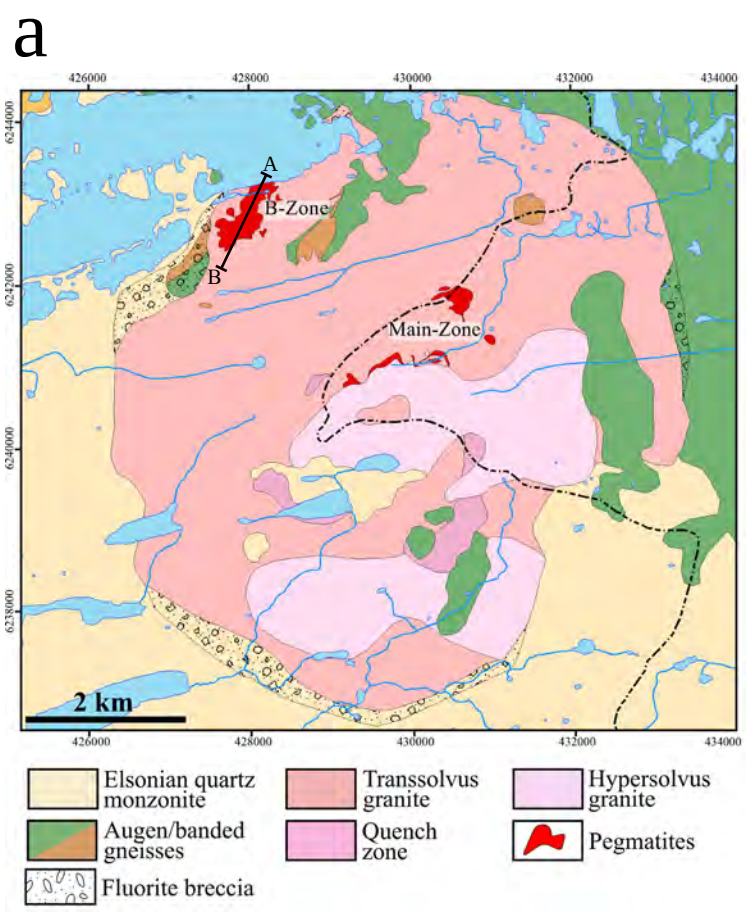

Figure 11 (a) – a geological map of the Strange Lake pluton modified from Vasyukova and Williams-Jones (2018) and (b) – a cross-section through the B-Zone pegmatites (indicated by the line A-B in (a)) modified from Gysi et al. (2016).

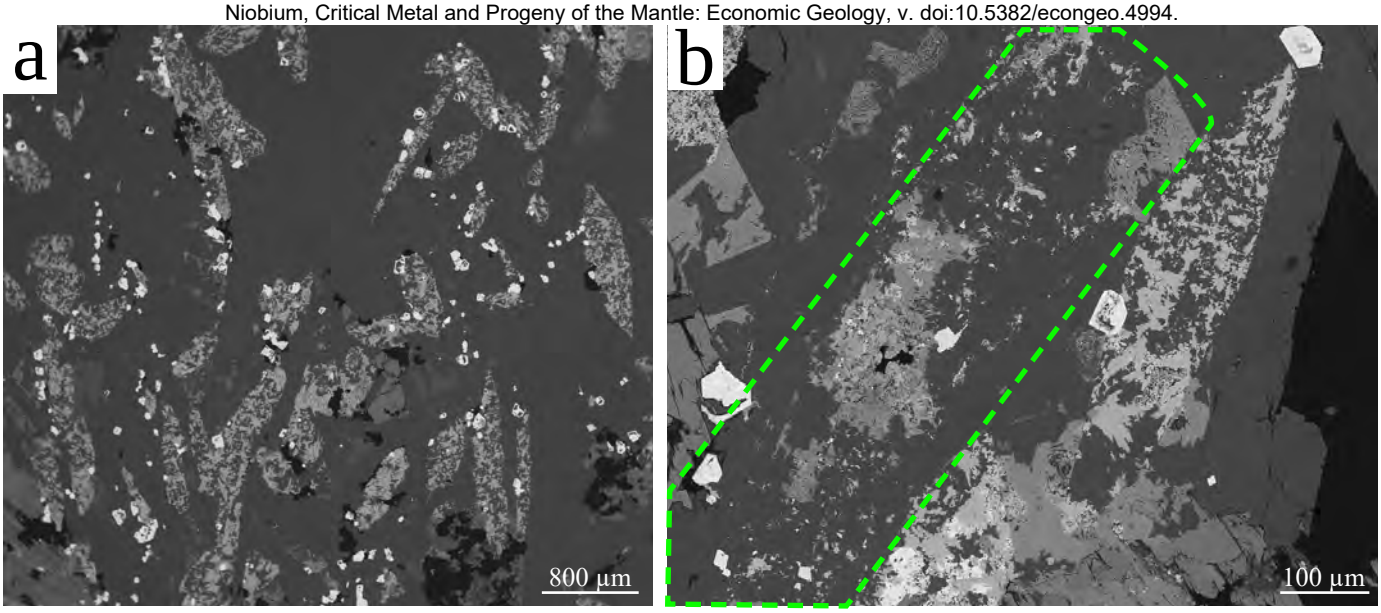

Figure 12 (a) - pseudomorphs of gittinsite (medium grey) and quartz (dark grey) after elpidite accompanied by crystals of pyrochlore (white) in a matrix of quartz. (b) - a pseudomorph of gittinsite and quartz with two associated crystals of pyrochlore and a pseudomorph (outlined by the green dashes) of titanite (medium grey) and quartz after narsarsukite containing several crystals of pyrochlore.

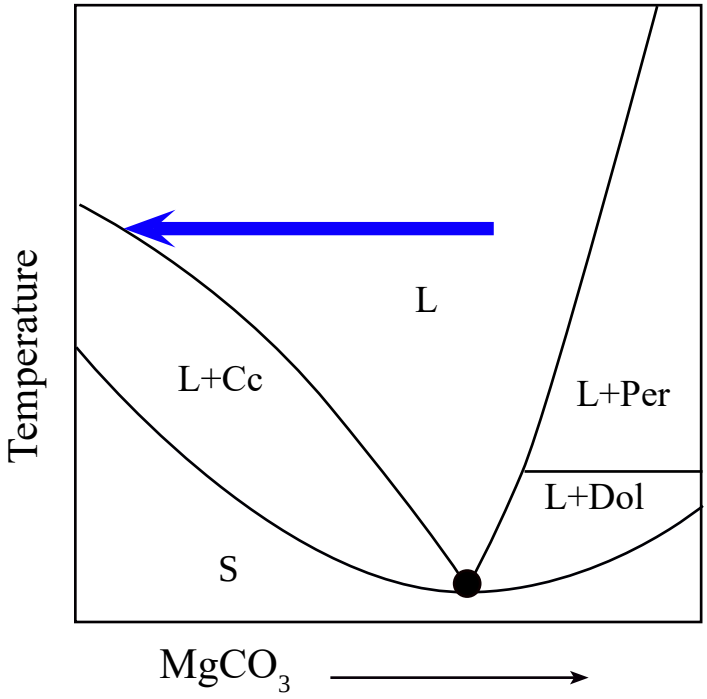

Figure 13 A schematic phase diagram showing relationships among liquid, calcite, dolomite and periclase in the system CaO-MgO-CO_2 as a function of temperature and the mole fraction of $MgCO_3$. The blue arrow indicates the displacement of the liquid composition to the calcite liquidus. See the main text for further detail. L – liquid, Cc – calcite, Dol – dolomite, Per – periclase and S – solid.

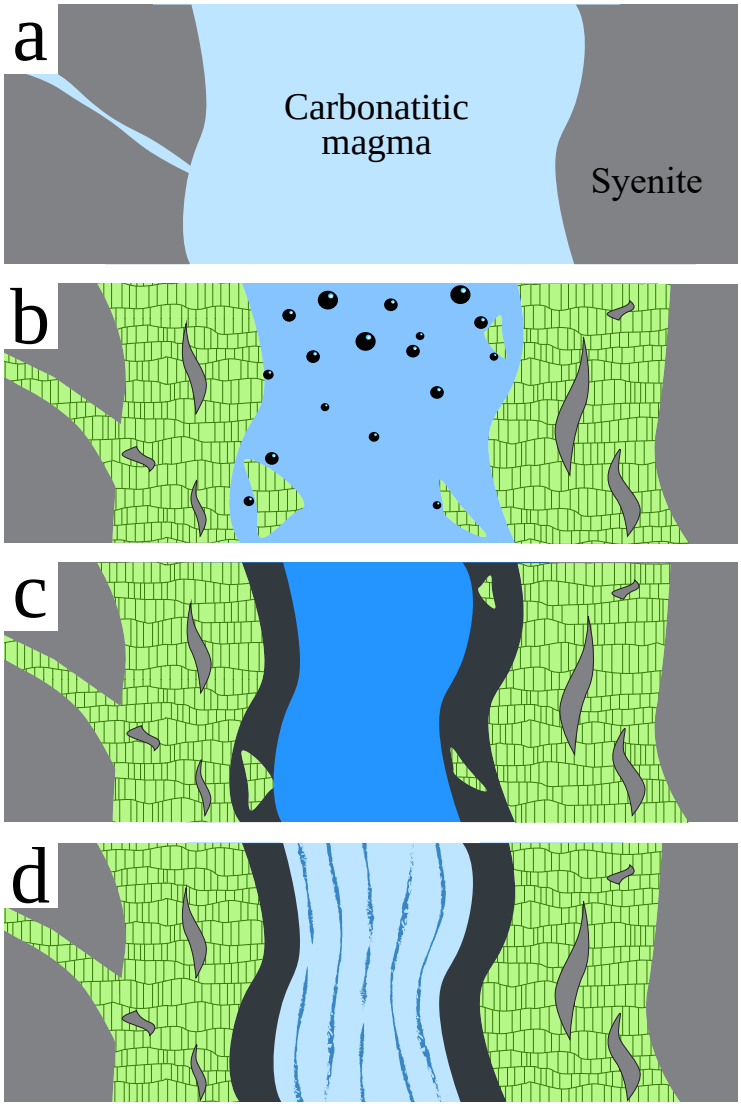

Figure 14 A cartoon illustrating the progressive interaction of a carbonatitic magma (dolomitic) with a syenite. (a) – the emplacement of the carbonatitic magma along fractures in K-feldspar-rich syenite; (b) – the alteration of K-feldspar by the carbonatitic magma to phlogopite (green), calcio-carbonatitic magma (medium blue) and CO_2 (bubbles); (c) – crystallization of calcite (dark grey) from the calcio-carbonatitic magma leaving a residual phoscoritic magma (dark blue) and (d) – incorporation of the residual phoscoritic magma as layers (dark blue) in a later batch of carbonatitic magma (light blue). See the main text for further detail.

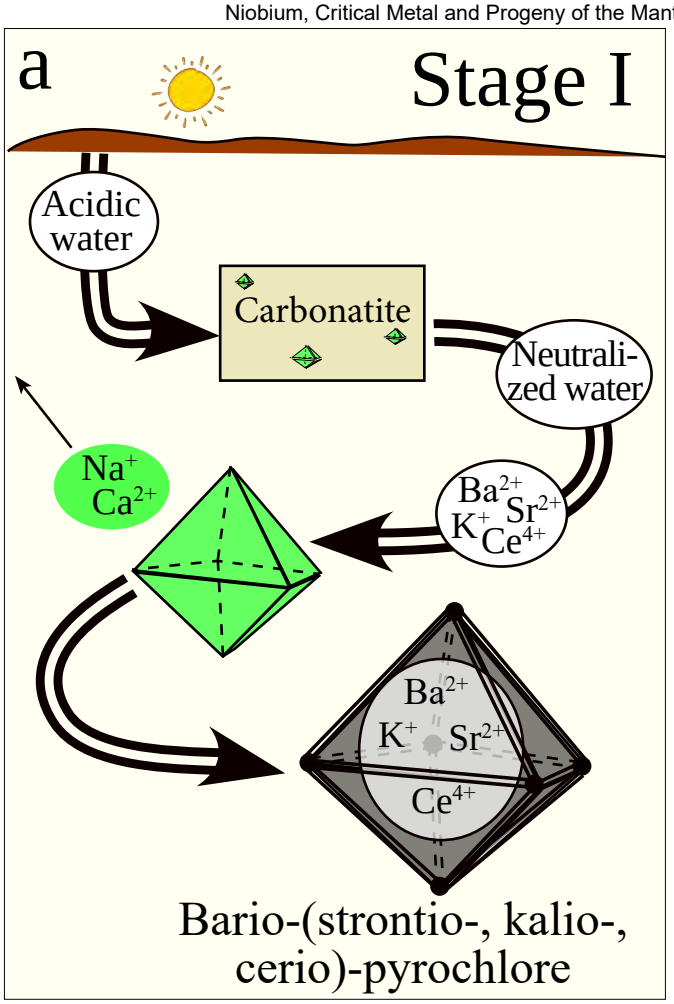

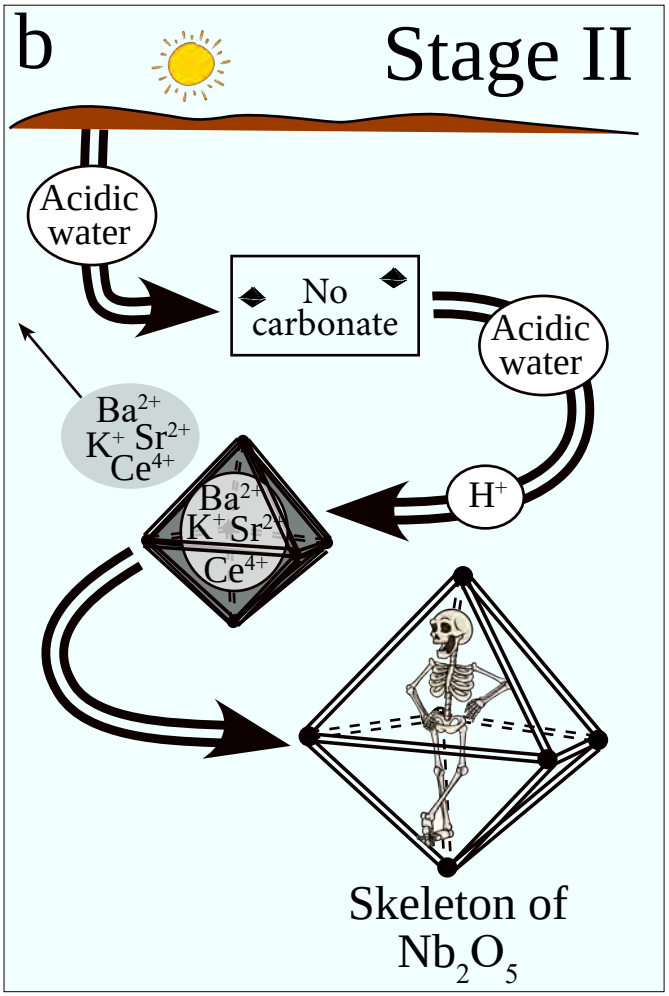

Figure 15 A two-stage cartoon showing the alteration of pyrochlore during weathering of carbonatite by mildly acidic meteoric water. (a) – Stage I, illustrating the dissolution of the carbonatite by early aliquots of the meteoric water, the release of Ba^{2+}, K^+, Sr^{2+} and Ce^{4+} to the neutralized water and the replacement of Na^+ and Ca^{2+} in the pyrochlore by these cations; (b) – Stage II, illustrating that in the absence of carbonatite (dissolved), further aliquots of meteoric water remain acidic and leach the A-site cations to yield a skeleton of Nb_2O_5. See the main text for further detail.

Williams-Jones, A. E., and Vasyukova, O. V., 2022,
Niobium, Critical Metal and Progeny of the Mantle: Economic Geology, v. doi:10.5382/econgeo.4994.

Table 1. Commonly reported niobium minerals and their chemical formulae.

Aeschynite-(Ce)	$(Ce,Ca,Fe,Th)(Ti,Nb)_2(O,OH)_6$
Baotite	$Ba_4(Ti,Nb)_8Si_4O_{28}Cl$
Charleshatchettite	$CaNb_4O_{10}(OH)_2.8H_2O$
Columbite-(Fe)	$Ee^{2+}Nb_2O_6$
Euxenite-(Y)	$(Y,Ca,Ce,U,Th)(Nb,Ta,Ti)_2O_6$
Fergusonite-(Y)	$YNbO_4$
Fersmite	$(Ca,Ce,Na)(Nb,Ta,Ti)_2(O,OH,F)_6$
Ixiolite	$(Ta,Nb,Sn,Fe,Mn)_4O_8$
Loparite-(Ce)	$(Na,Ce,Ca)(Ti,Nb)O_3$
Lueshite	$NaNbO_3$
Ilmenorutile**	$(Ti,Nb)O_2$
Niobian Brookite	$(Ti,Nb)O_2$
Niocalite	$Ca_7Nb(Si_2O_7)_2O_3F$
Pyrochlore*	$(Ca,Na)_2O_6F$
Samarskite-(Yb)	$(Yb,Y,U,Th,Ca,Fe)(Nb,Ta)O_4$
Tapiolite	$(Fe,Mn)(Ta,Nb)_2O_6$
Wodginite	$(Ta,Nb,Sn,Fe)_{16}O_{32}$

*Pyrochlore is a group of minerals with a complex chemistry described by the formula $A2\text{-}mB_2X_{6\text{-}w}Y_{1\text{-}n}$, The A and B sites can accommodate a large number of elements and a vacancy, the X sites is typically occupied by O but can also contain OH^- and F^-, and the Y site can contain OH^-, F^-, Cl, H_2O, a large cation and be vacant. The formula listed here is for fluorcalciopyrochlore, which in the rest of the paper, we refer to as calcio-pyrochlore (see main text for further information).

** Ilmenorutile is referred to in the manuscript as niobian rutile.

Williams-Jones, A. E., and Vasyukova, O. V., 2022,
Niobium, Critical Metal and Progeny of the Mantle: Economic Geology, v. doi:10.5382/econgeo.4994.

Table 2. The evolution of the niobium concentration of carbonatitic and alkaline silicate magmas after partial melting of primitive and enriched mantles, initially containing 0. 6 and ~ 2 ppm Nb, respectively.

Process	Carbonatitic magma		Silica-undersaturated alkaline silicate magma		Silica-saturated alkaline silicate magma	
	Percent process	Niobium (ppm)	Percent process	Niobium (ppm)	Percent process	Niobium (ppm)
Partial melting (primitive mantle)	0.5	120	2	30	2	30
Partial melting (enriched mantle)	0.5	300	2	100	2	100
Fractional crystallization (parental magma)			72	350	67	300
Fractional crystallization (to ore grade)			84	2,200	86	2,100